

# Status and perspectives of the QUAX-LNL 10 GHz axion haloscope



Raffaele Di Vora

Laboratori Nazionali di Legnaro (Italy)  
(on behalf of the QUAX collaboration)

Slides mutated & readapted from G.Ruoso's talk in Rome on 12.05.2026

# The axion

The axion is a **light pseudoscalar boson**, introduced in the 70s to solve the strong CP problem (Peccei and Quinn 1977)

$$m_a = 5.70(6)(4) \mu\text{eV} \left( \frac{10^{12}\text{GeV}}{f_a} \right)$$

- $f_a$  is the axion decay constant, related to the scale of spontaneous breaking of the PQ symmetry
- the strong CP problem is solved regardless of the value of  $f_a$
- $f_a$  is the quantity that determines all the low energy phenomena of the axion

**Axion couplings** with ordinary matter depends on the model implementing the PQ symmetry

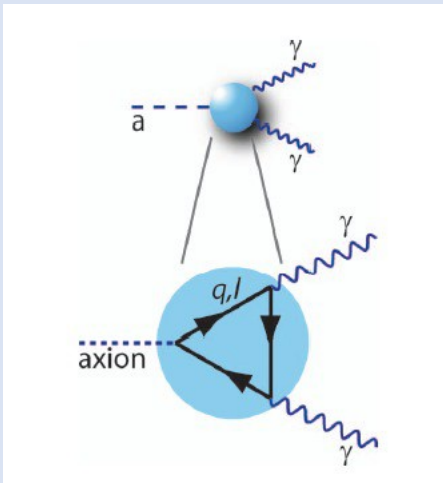
**Axion photon**

$$\mathcal{L}_{a\gamma\gamma} = - \left( \frac{\alpha}{\pi} \frac{g_\gamma}{f_a} \right) a \vec{E} \cdot \vec{B} = -g_{a\gamma\gamma} a \vec{E} \cdot \vec{B}$$

**[Axion nucleon]**

**Axion electron**

$$L_{aee} = -g_e \bar{e} i \gamma_5 e a$$



$$g_\gamma = 0.36 \text{ (DFSZ)}$$

$$g_\gamma = -0.97 \text{ (KSVZ)}$$

$$g_e \approx \frac{m_a m_e}{m_\pi f_\pi} = 4.07 \times 10^{-11} m_a \text{ (DFSZ)}$$

$$g_e \sim 0 \text{ (Strongly suppressed) (KSVZ)}$$

KSVZ – Kim 1979, Shifman-Vainshtein-Zakharov 1980

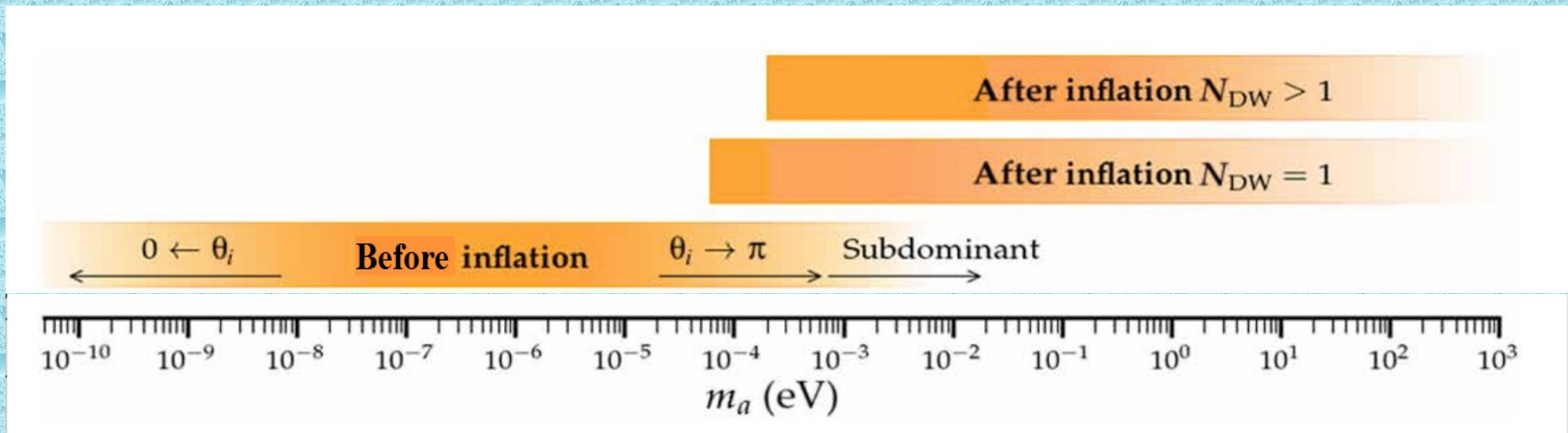
DFSZ – Dine-Fischler-Srednicki 1981, Zhitnitsky 1980

# Dark matter axion

- Non-thermal mechanisms in the early Universe could have produced axions: the *vacuum realignment mechanism* and the *decay of topological defects* (axion strings and domain walls) → **Cold dark matter (GOOD)**
- *Vacuum realignment mechanism*: relaxation of the axion field after breakdown of the PQ symmetry → The expected cosmic mass density of axions depends on whether **inflation happens after or before PQ breakdown**

Allowed regions of mass  
(decay constant)

- These regions obtained by **assuming axion saturate DM density**. Lower values of  $m_a$  would overproduce DM while higher masses would lead to subdominant amount of axion DM
- If axions exist at least a fraction of DM are axions



# The pre- and post- inflationary scenarios

Difference between the pre- and post- inflationary scenarios is **predictability**:

- In **pre-inflationary** there are **two continuous free parameters**, an angle  $\theta$  and the mass  $m_a$ , to obtain the observed dark matter density
- In **post-inflationary** there is one continuous parameter,  $m_a$ , and a discrete one  $N$ .
  - In principle the observed DM density predicts the value of  $m_a$
  - Due to nonlinearities, computing this mass accurately is a real challenge
  - Recent works make use of large static lattice simulations

SciPost Select SciPost Phys. 10, 050 (2021)

**More axions from strings**

Marco Gorghetto<sup>1</sup>, Edward Hardy<sup>2</sup> and Giovanni Villadoro<sup>3</sup>

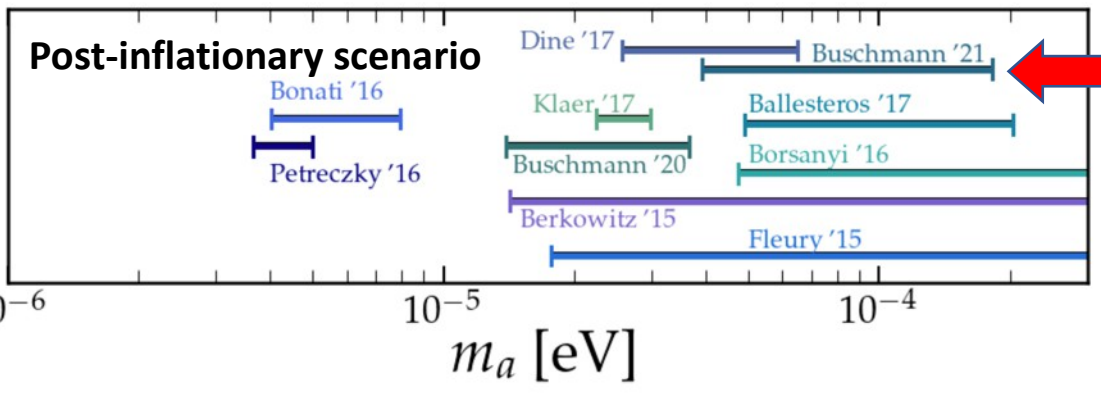
*Nature Communications* volume 13, Article number: 1049 (2022)

ARTICLE Check for updates

<https://doi.org/10.1038/s41467-022-28669-y> OPEN

## Dark matter from axion strings with adaptive mesh refinement

Malte Buschmann<sup>1✉</sup>, Joshua W. Foster<sup>2,3,4✉</sup>, Anson Hook<sup>5</sup>, Adam Peterson<sup>6</sup>, Don E. Willcox<sup>6</sup>, Weiqun Zhang<sup>6</sup> & Benjamin R. Safdi<sup>3,4✉</sup>



$m_a \approx (40, 180) \mu\text{eV}$

# The source - Axions in the galactic halo

- In order to explain galaxy rotation curves, a **halo of dark matter** is hypothesized

- Accepted value for local dark matter **density**

$$\rho_{DM} \approx 0.3 - 0.45 \text{ GeV/cm}^3$$

- Cold dark matter component is **thermalized** and has a Maxwellian velocity distribution, with a dispersion  $\sigma_v \approx 270 \text{ km/s}$
- There might be a non-thermalized component with sharper velocity distribution



- **Axion can be a dominant component of the galactic DM halo**

- Its **occupation number** is large

$$n_a \approx 3 \times 10^{14} \left( \frac{10^{-6} \text{ eV}}{m_a} \right) \text{ axions/cm}^3$$

- It can be treated as a classical oscillating field with frequency given by the axion mass

$$\frac{\omega_a}{2\pi} = 2.4 \left( \frac{10^{-6} \text{ eV}}{m_a} \right) \text{ GHz}$$

$$\lambda = 1400 \left( \frac{10^{-6} \text{ eV}}{m_a} \right) \text{ m}$$

- It has **coherence length** and **time**

$$t = 5 \left( \frac{10^{-6} \text{ eV}}{m_a} \right) \text{ ms}$$

# Haloscopes – Galactic axions – Sikivie Type

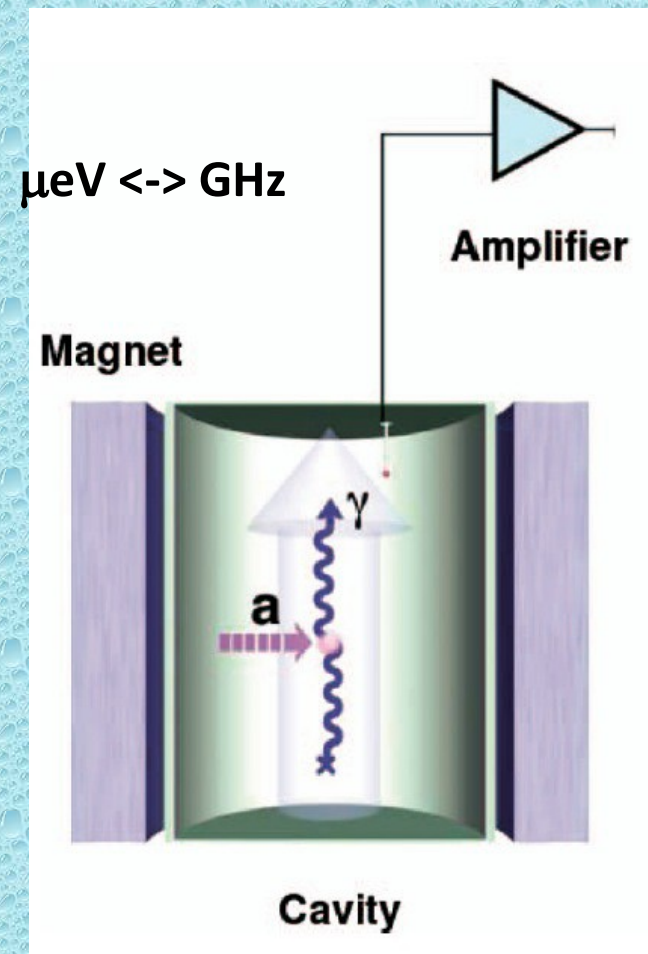
- Search for axions as cold dark matter constituent exploiting **axion – photon coupling**
- Original proposal by P. Sikivie (1983)
- **DM particles converted into photons inside a magnetic field (inverse Primakoff effect), sensitivity to  $g_{a\gamma\gamma}$**

- **The mass of the DM particle determines the frequency of the photons to be detected. For axions we are in the microwave range.**

$$h\nu = E_a = m_a c^2 \left( 1 + \frac{1}{2} \beta_a^2 \right) = m_a c^2 (1 + O(10^{-6}))$$

$\beta_a \sim 10^{-3}$  axion velocity

- **Use a microwave cavity** to enhance signal. Cavity must be tuned to axion mass. Being this unknown, **tuning is necessary**: very time consuming experiment!



# Haloscopes – Galactic axions

- Search for axions as cold dark matter constituent exploiting **axion – photon coupling**
- Original proposal by P. Sikivie (1983)
- **DM particles converted into photons inside a magnetic field (Primakoff)**
  - Expected signal a **nearly monochromatic line**. Broadened by the **thermal distribution** of DM in the Milky Way

$$\beta_a^2 \sim 10^{-6} = 1/Q_a$$

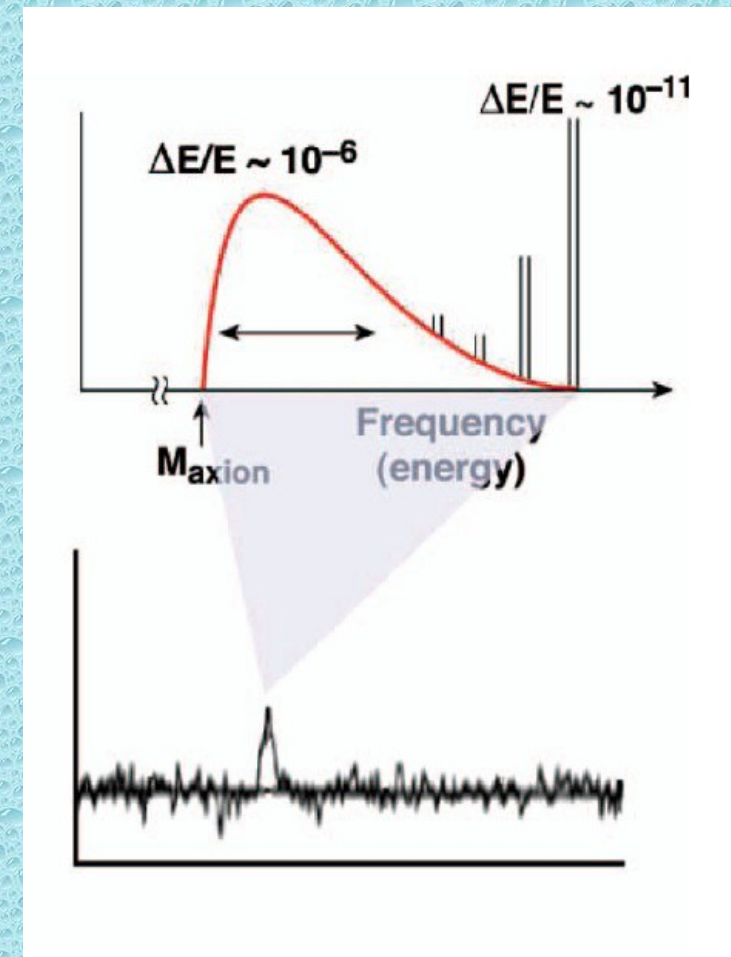
- Possible **very sharp component due to non-thermalised** axion falling in and out of the Milky Way

$$Q_{streams} \sim 10^{11}$$

- **Power** proportional to the number density and the square of the axion-photon coupling

$$P_a = \frac{g_{a\gamma\gamma}^2 \rho_a}{m_a} B_0^2 V C \frac{\beta}{(1 + \beta)} \frac{Q_L Q_a}{Q_L + Q_a}$$

- Typical powers to be measured below  $10^{-23}$  W



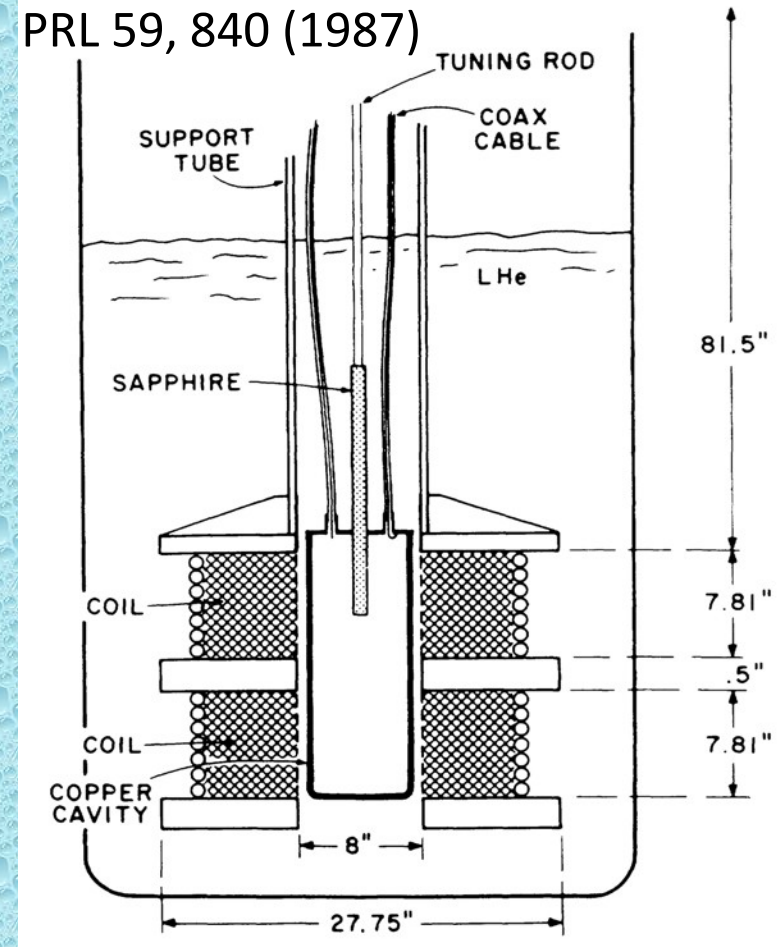
# Haloscopes – Galactic axions

- Resonant detection of DM axions in a magnetic field. One measurement explores **only sharp cavity linewidth**. **Scanning** is necessary.

Figure of merit for scanning (mass or frequency)

$$\frac{\Delta f}{\Delta t} \propto V^2 B^4 C^2 T_{sys}^{-2} Q$$

- High Q** microwave cavity operating inside a **strong magnetic field B**
- Large volume V** cavity at **high RF frequency f**
- Low noise  $T_{sys}$**  radio frequency receiver
- Use cavity modes with **large form factor C**



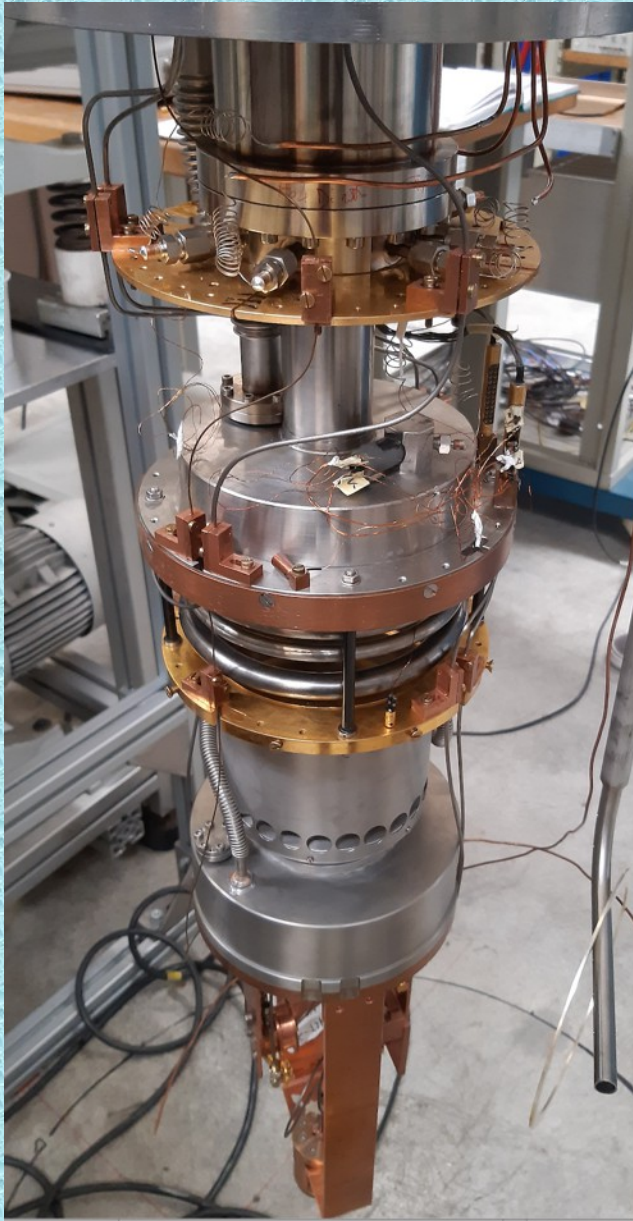
Schematic diagram of the RBF apparatus (1987)

- Scanning to high mass – high frequency very difficult due to reduced cavity volumes
- Scanning to low mass – low frequency implies large cavities and thus very big magnets

**! All current limits assumes axion/ALPs saturate the local DM density**

# Main components of cavity haloscopes

Refrigeration system



Base temperature  $T$

Microwave cavity



Quality Factor  $Q_c$

Form factor  $C_{mnl}$

Volume  $V$

Resonance frequency  $f$

Tuning

Magnetic source

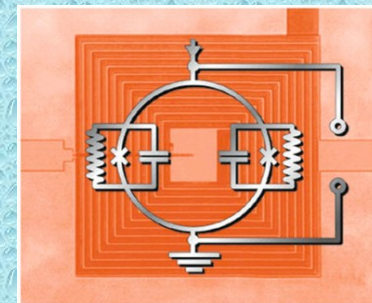


Magnetic energy  $B^2 V$

Low noise receiver

(Picture and scheme of a SQUID)

Noise temperature  $T_n$



# Sensitivity

When the frequency of the axion induced photon matches the frequency of the **cavity eigenmode**, the conversion power is **resonantly enhanced** via cavity  $Q_c$  ( $Q_c \ll Q_a$ )  $Q_L = Q_c / (1 + \beta)$

$$P_{\text{axion}} = 1.1 \times 10^{-23} \text{ W} \left( \frac{g_\gamma}{1.92} \right)^2 \left( \frac{\rho_a}{0.45 \text{ GeV/cm}^3} \right) \left( \frac{\nu_a}{1 \text{ GHz}} \right) \left( \frac{B_0}{10 \text{ T}} \right)^2 \left( \frac{V}{1 \text{ liter}} \right) \left( \frac{C_{mnl}}{0.69} \right) \left( \frac{Q_L}{10^5} \right) \frac{\beta}{(1 + \beta)}$$

The **power is picked up by an antenna** with coupling  $\beta$  and read by an amplifier. Extremely low power levels are detected by sensitive amplifiers

In the absence of a signal, the output of a receiver is noise, measured on a **bandwidth  $B_a$**  corresponding to the axion linewidth

$$P_{\text{noise}} = Gk_B(T_{\text{cav}} + T_{\text{ampl}})B_a = Gk_B T_{\text{sys}} B_a$$

Cavity noise + amplifier noise

$T_{\text{ampl}}$  = amplifier noise temperature

$G$  – gain ;  $k_B$  – Boltzmann constant

$T_{\text{sys}}$  = total system noise temperature

The **SNR** can be calculated with **Dicke's radiometer equation** for a **measurement time  $t_m$**

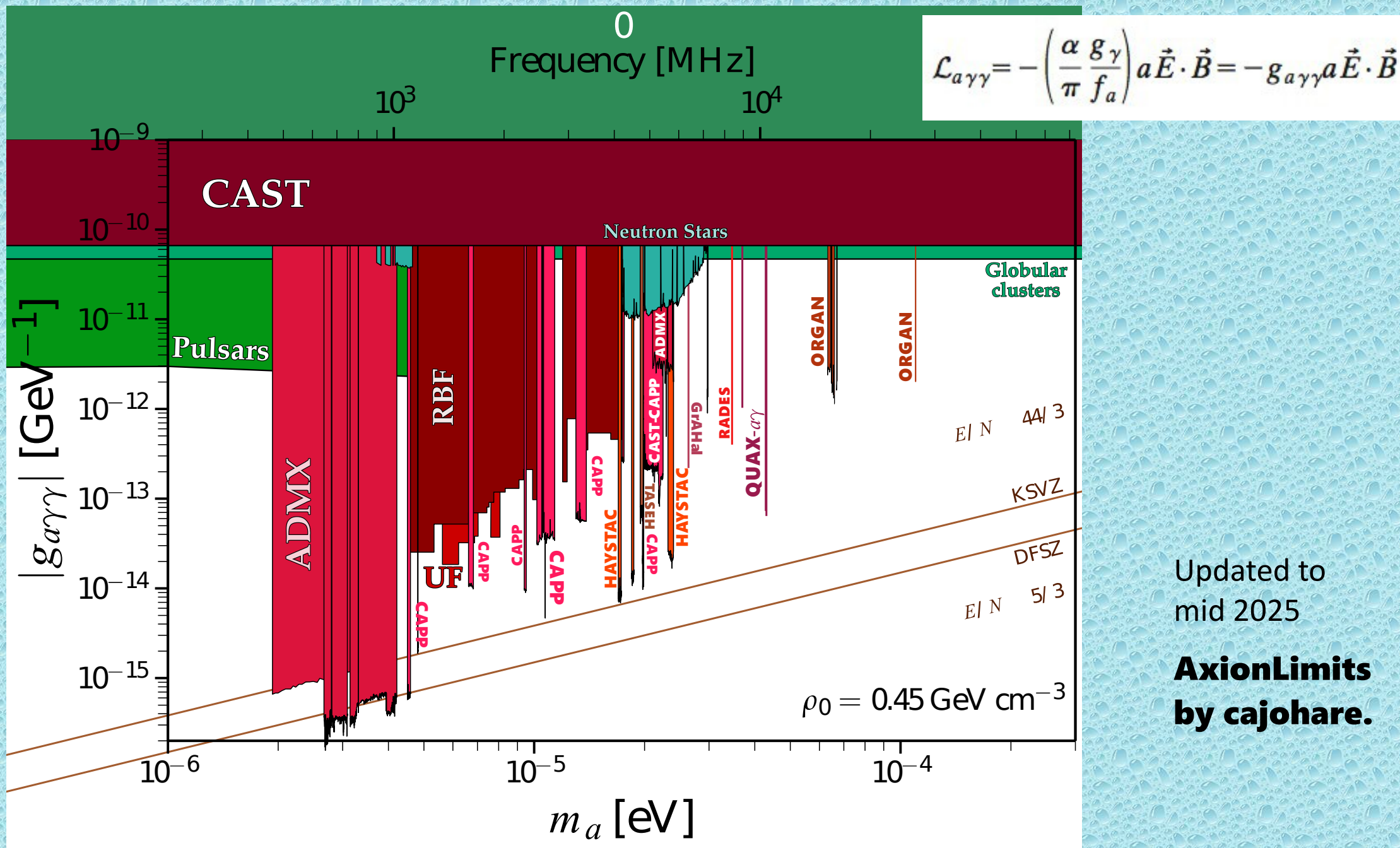
$$\text{SNR} = \frac{P_{\text{axion}}}{k_B T_{\text{sys}}} \sqrt{\frac{t_m}{B_a}}$$

Since all the frequencies within a cavity bandwidth can be scanned simultaneously, we can calculate a **scanning rate** as

$$\frac{df}{dt} = \frac{1}{\text{SNR}^2} \frac{P_{\text{axion}}^2}{k_B^2 T_{\text{sys}}^2} \frac{Q_a}{Q_L}$$

Major R&D efforts are made to **increase  $B_0^2 V C_{mnl} Q_c$**  and **minimizing  $T_{\text{sys}}$**

# 2025 Limits – Sikivie’s haloscopes



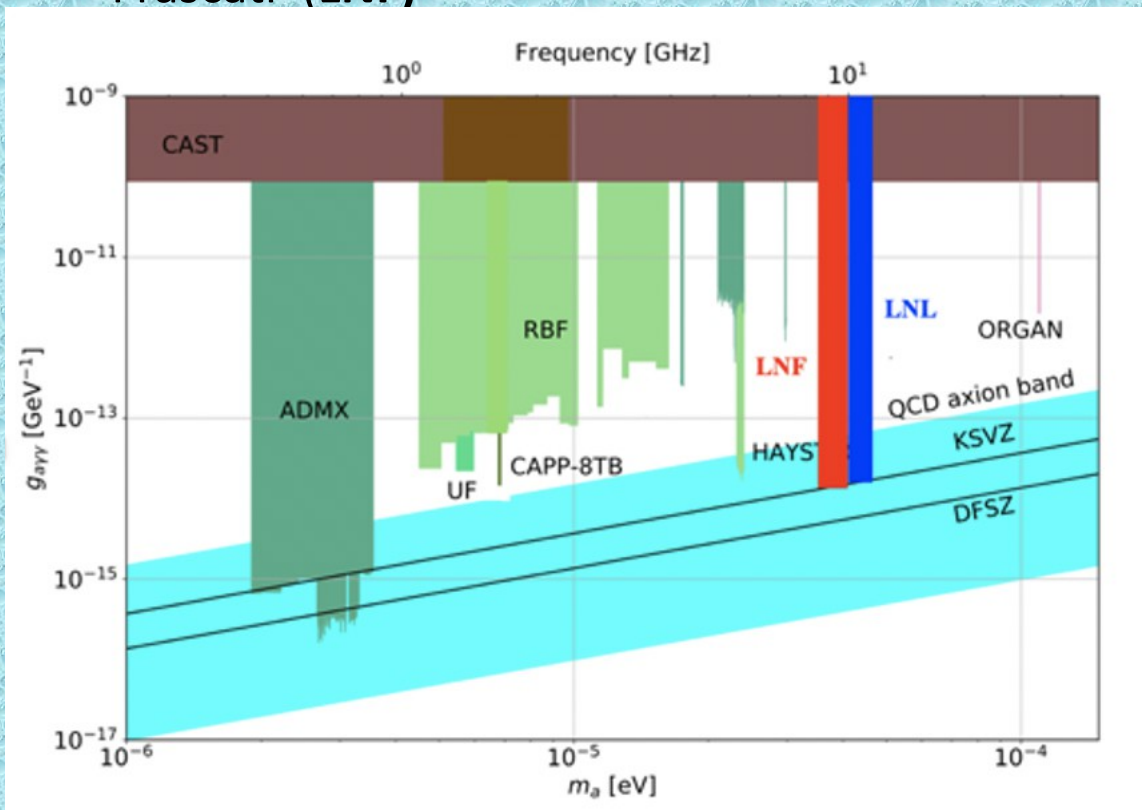
Updated to  
mid 2025

**AxionLimits  
by cajohare.**

# QUAX – QUaerere AXion – QUest for AXion

- In 2020 INFN has financed the **QUAX experiment** to run an observatory for searching axion via the **axion-photon coupling in the unexplored region around 10 GHz**

- QUAX is based on two haloscopes: one in Legnaro/Padova (LNL) and the other in Frascati (LNF)**



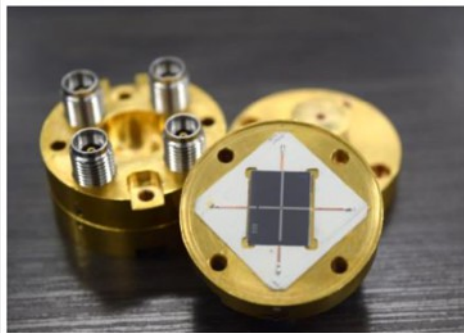
	LNF	LNL
Magnetic field	9 T	14 T
Magnet length	40 cm	50 cm
Magnet inner diameter	9 cm	12 cm
Frequency range	8.5 - 10 GHz	9.5 - 11 GHz
Cavity type	Hybrid SC	Dielectric
Scanning type	Inserted rod	Mobile cylinder
Number of cavities	7	1
Cavity length	0.3 m	0.4 m
Cavity diameter	25.5 mm	58 mm
Cavity mode	TM010	pseudoTM030
Single volume	$1.5 \cdot 10^{-4} \text{ m}^3$	$1.5 \cdot 10^{-4} \text{ m}^3$
Total volume	$7 \otimes 0.15 \text{ liters}$	0.15 liters
$Q_0$	300 000	1 000 000
Single scan bandwidth	630 kHz	30 kHz
Axion power	$7 \otimes 1.2 \cdot 10^{-23} \text{ W}$	$0.99 \cdot 10^{-22} \text{ W}$
Preamplifier	TWJPA/INRIM	DJJAA/Grenoble
Operating temperature	30 mK	30 mK

- The **LNL/PD haloscope** will be based on dielectric loaded cavities, traveling wave parametric amplifiers and 14 T magnet

# QUAX – Selection of past achievements

**Operation of a ferrimagnetic haloscope** to study axion-electron coupling ( $\rightarrow$  see supplementary material @End of Talk)

Operation of a quantum limited **JPC** at high frequency (10 GHz)

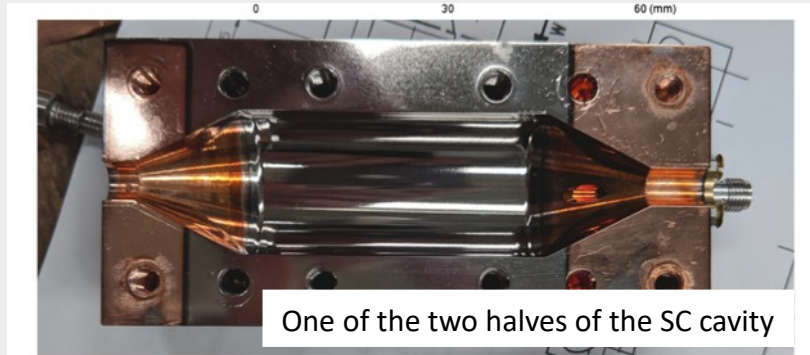


1 cm

Josephson  
Parametric  
Converter

$T_{\text{sys}} = 1\text{K}$

**First use of a superconducting cavity** in a strong magnetic field  $Q_0 = 4.5 \cdot 10^5 @ 2\text{ T}$



One of the two halves of the SC cavity

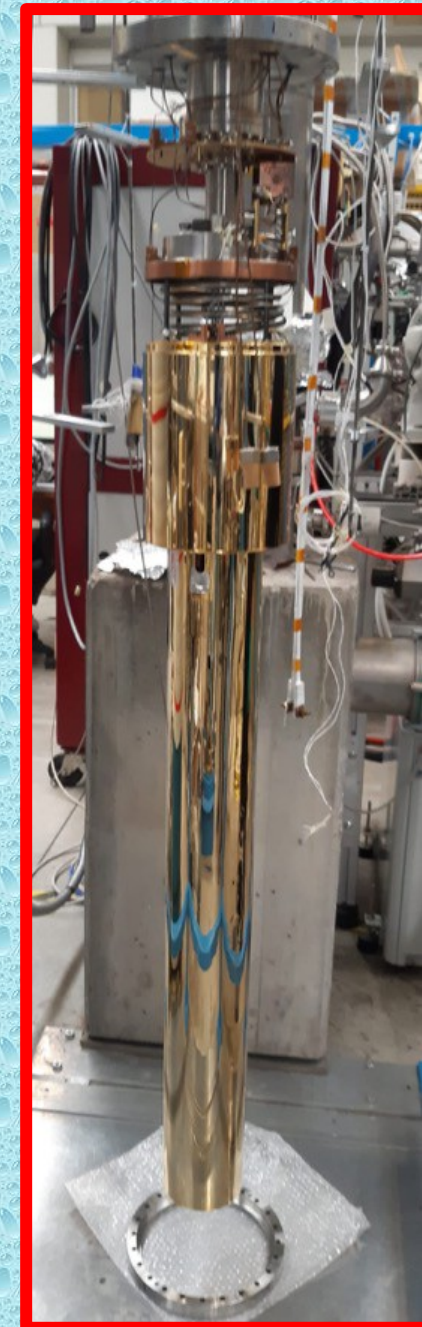
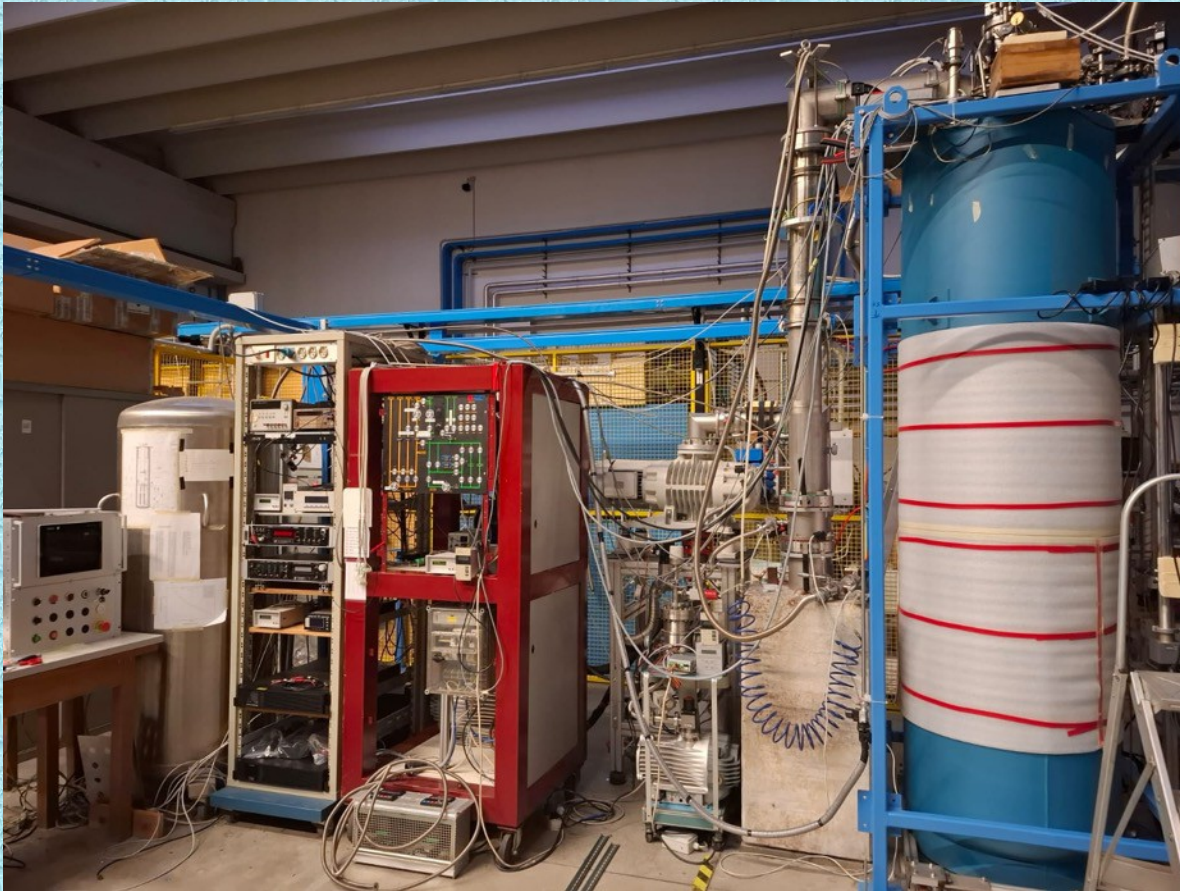
Use of **hybrid cavity design (copper-sapphire)** to get high  $Q$  and large volume

First haloscope employing a cavity with  $Q_c \approx 10^7 > Q_a$  !

**TODAY  $\rightarrow$  Recent results with the QUAX haloscope of Legnaro/Padova**

# Refrigeration system

QUAX main criostat with gas handling system and safety control



Gold Plated  
heat shield

- Main dewar: 2800 mm height, 500 mm inner diameter
- Two weeks operation: ~ 3000 liters of liquid Helium
- Refurbished **wet dilution unit** from AURIGA experiment
- Base temperature @ MC 60 mK
- **Cavity and electronics kept @ 120 mK**

# Dielectrically loaded tunable cavity – single sapphire

Right cylindrical hybrid cavity  
TM<sub>030</sub> mode for large volume  
Copper shell  
Hollow Sapphire cylinder inside

Clamshell mechanism for tuning

Base frequency 10.2 GHz

$$C = \frac{|\int_V d^3r \mathbf{E}_{\text{nml}} \cdot \mathbf{B}|^2}{\int_V d^3r |\mathbf{B}|^2 \int_V d^3r \epsilon_r(\mathbf{r}) |\mathbf{E}_{\text{nml}}|^2}$$

**LAMED TC**

(Phoenician: Goad)



Inner length = 413.4 mm  
Inner diameter = 60.5 mm  
Volume = 1.17 liters

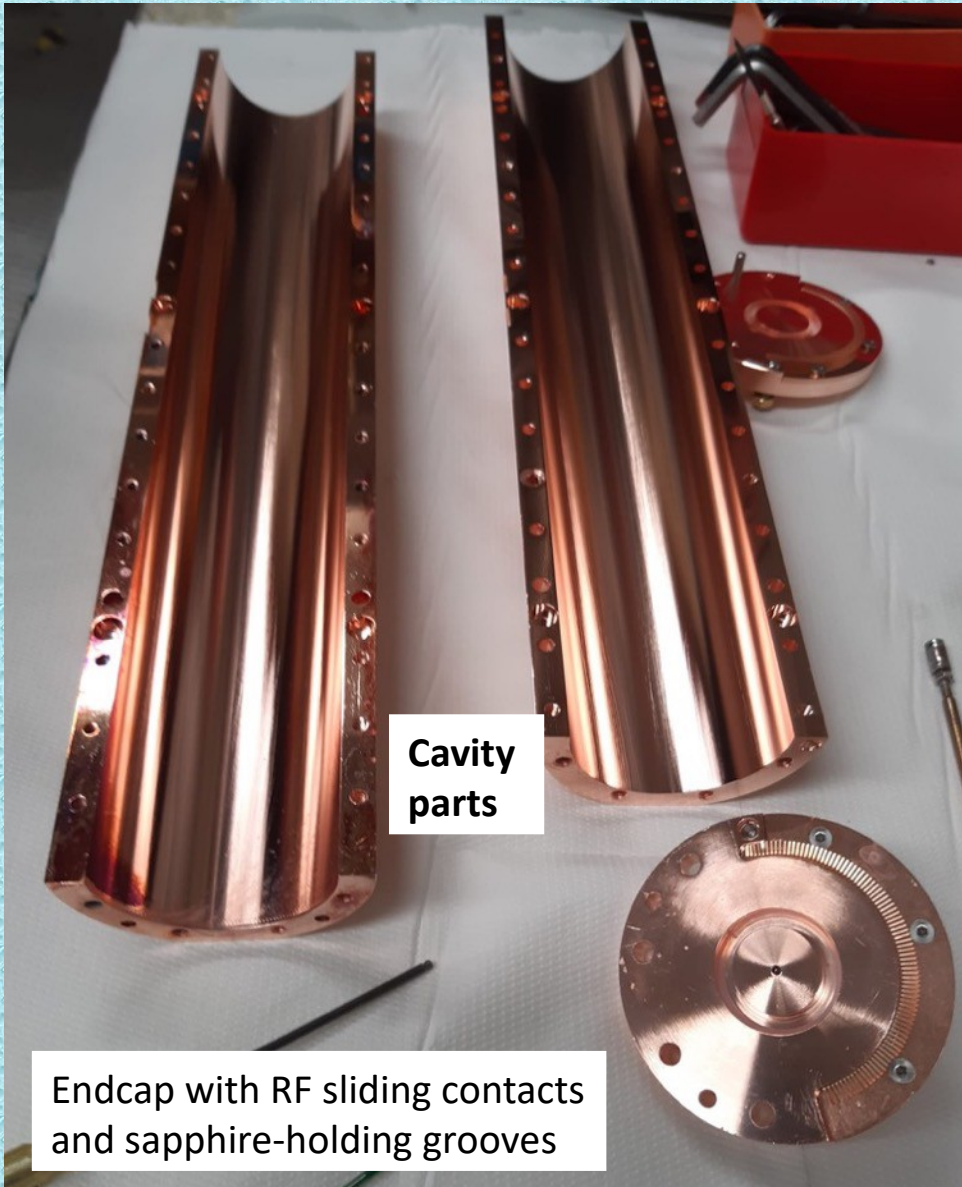
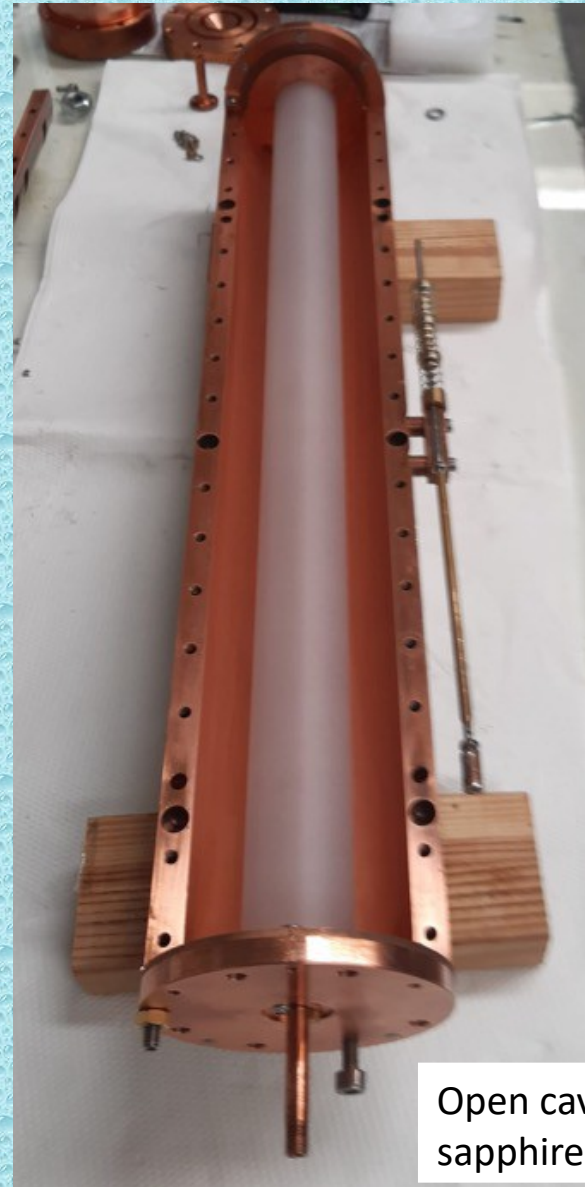
Tunable coupling  
RF Antenna



Open cavity with  
sapphire cylinder

Cavity  
parts

Endcap with RF sliding contacts  
and sapphire-holding grooves



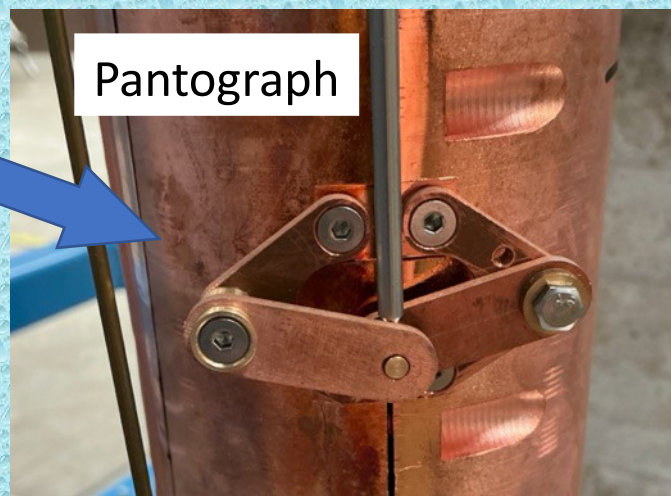
# Dielectrically loaded tunable cavity – single sapphire

**LAMED TC**

(Phoenician: Goad)



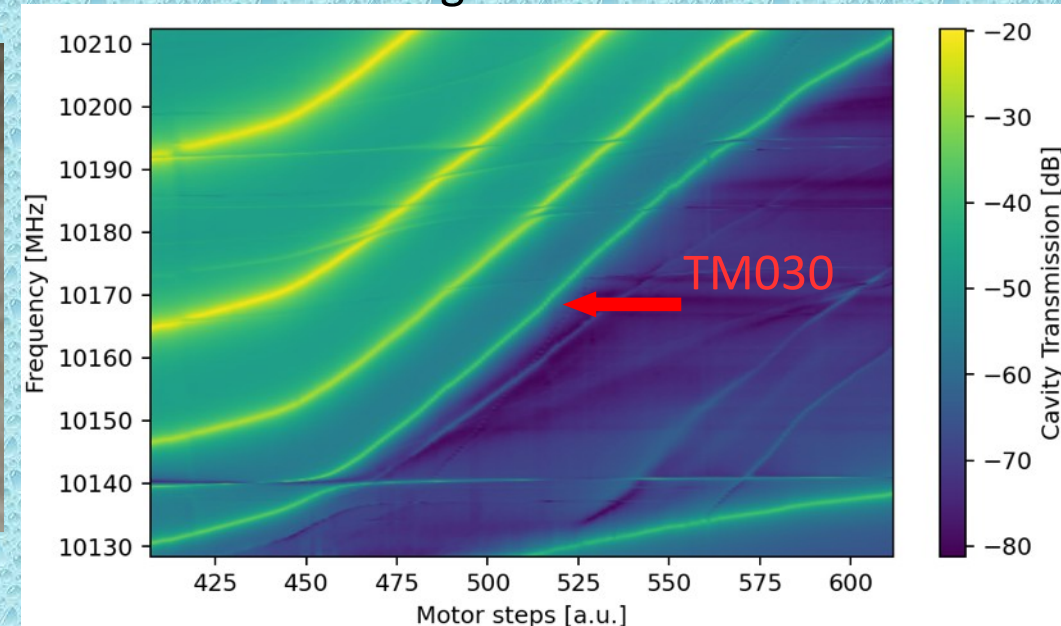
- Material OFHC Copper
- L = 420 mm sapphire cylinder (from Armenia)
- Movable side wall - clamshell mechanism
- Single body endcaps
- Endcaps with 5.3 mm deep grooves for sapphire holding and radial centering
- Copper RF sliding gaskets
- Motor actuated pantograph-like aperture mechanism
- Teflon 1.1 mm diameter for sapphire z centering
- **science mode TM030**
- **Total tuning 85 MHz (10.212 to 10.126 GHz)**
- **$Q_0 \sim 80\,000$**



Inner length = 413.4 mm  
Inner diameter = 60.5 mm

Volume = 1.17 liters,  $C_{030} = 0.43$

Tuning



# Magnetic field



- Counter field magnet, NbTi superconducting coil
- Inner diameter 150 mm, height 250 mm
- Same driving current of main magnet
- Reduces stray field below 40 mT on sensitive electronics (passively shielded too!)

- Main magnet, NbTi superconducting coil
- 450 mm length, 150 mm inner diameter
- **Peak field 8.0 T @ 92 A current**
- Mean square field in cavity volume 50.2 T<sup>2</sup>

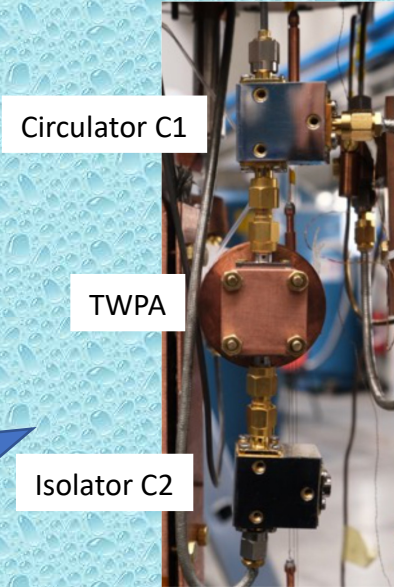
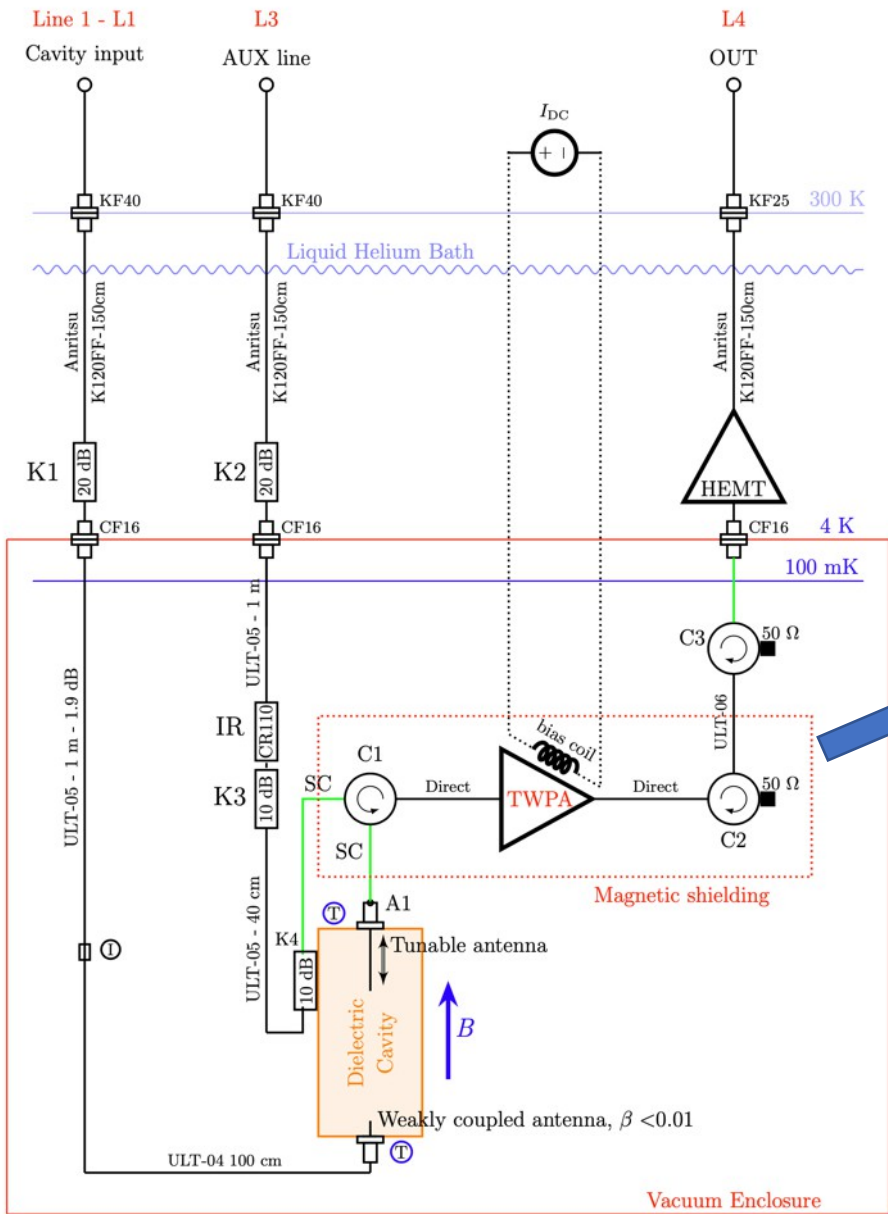
# RF Receiver

High frequency receiver working in a strong magnetic field environment

The 10 GHz low noise receiver is based on a **Traveling Wave Parametric Amplifier (TWPA** - from N. Roch (Grenoble))

A. Ranadive, et al., Nat. Commun. 13, 1737 (2022)

(a) Radio Frequency Cryogenic layout May 2024



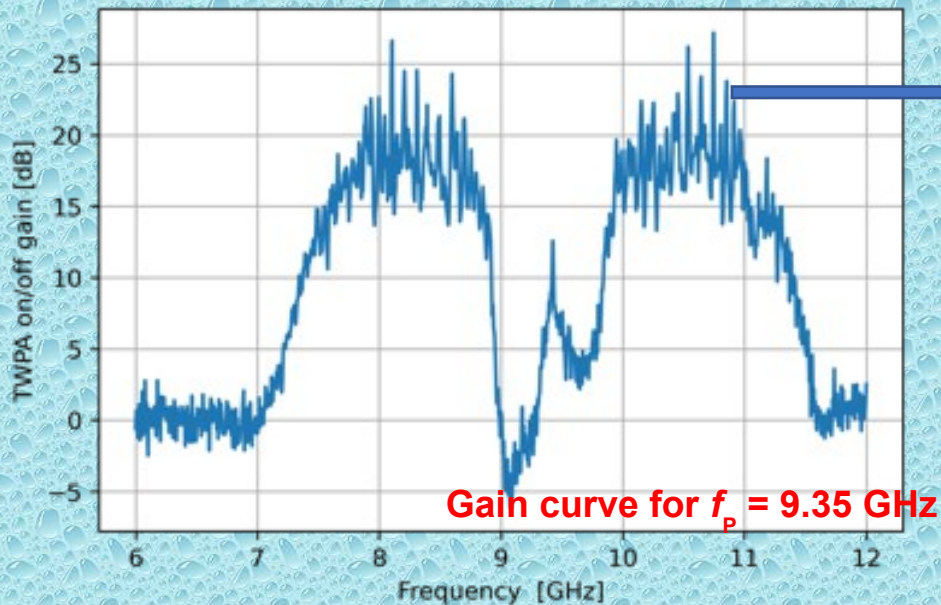
Magnetic shielding (grey box)

TWPA is made by **superconducting Aluminum** Josephson Junction arrays very sensitive to ambient magnetic field  
Two-layers passive shielding: **CRYOPERM (inside) + lead**

# TWPA Amplifier set-up

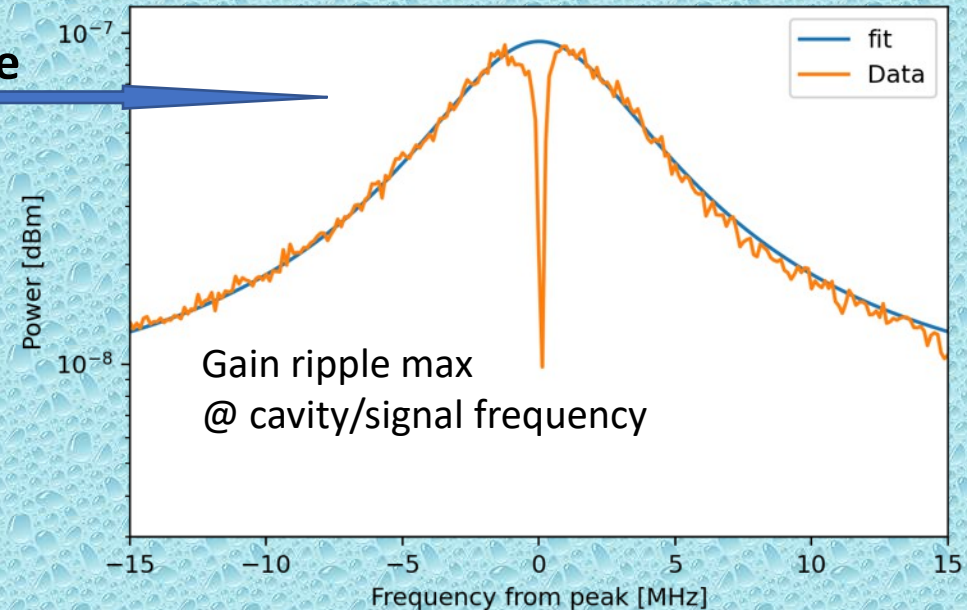
- **four wave mixing TWPA** with a phase matching process based on the sign reversal of the third order (Kerr) nonlinearity of a series of Josephson Junctions arrays (A. Ranadive, et al., Nat. Commun. 13, 1737 (2022) )
- TWPA amplification controlled by **intensity  $I_p$**  and **frequency  $f_p$**  of the pump tone and **current  $I_b$**  of a biasing magnetic field

(a) TWPA ON/OFF Gain

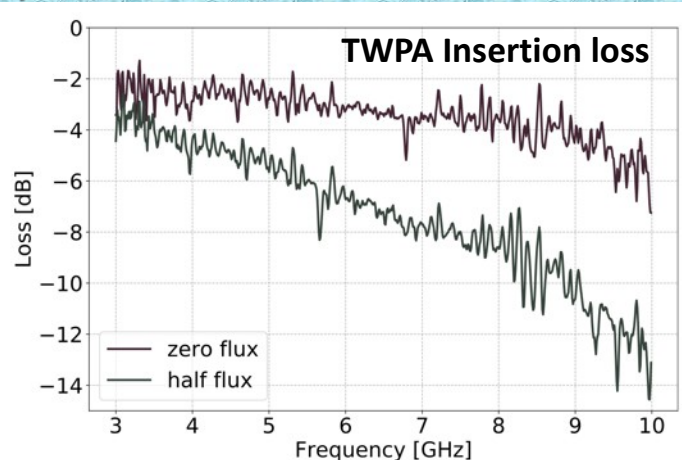


Single ripple

In order to maximize SNR one has to tune the gain profile of the TWPA amplifier



High frequency operation has to cope with large IL that reduces effective gain



Measured Noise Temperature

$$T_{\text{sys}} = 1.1 \text{ K @ } 10.2 \text{ GHz}$$

$$T_{\text{sys}} = 0.8 \text{ K @ } 7.9 \text{ GHz}$$

-> ~ 2.3 Photons

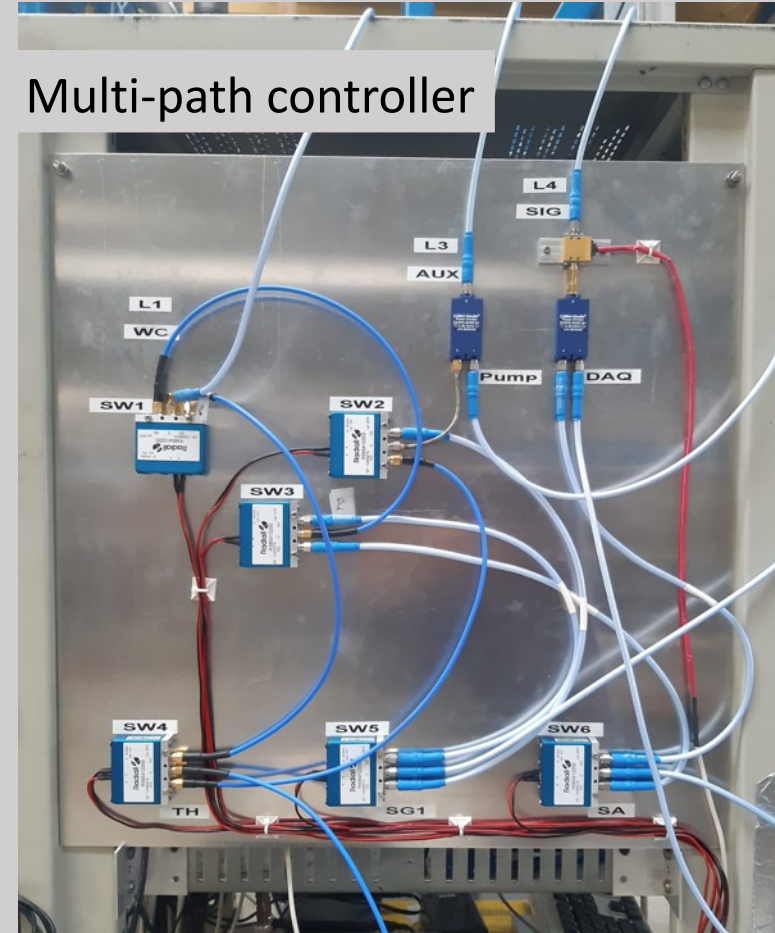
# Run control

## Run steps:

1. Cavity tuning (5 m)
2. TWPA amplifier set (0s [autom.]/some minutes [manual])
3. Measurement of Tsys and Gain (2 m)
4. Measurement of  $f_c$ , QL, Q0, gain profile (2 m)
5. Short data acquisition with thermal input (2 m)
6. Repeat steps 3-4 (4 m)
7. Long data acquisition with no input (65 m)
8. Repeat steps 3-4 (4 m)
9. Start over

Time for a single point 80 - 100 minutes

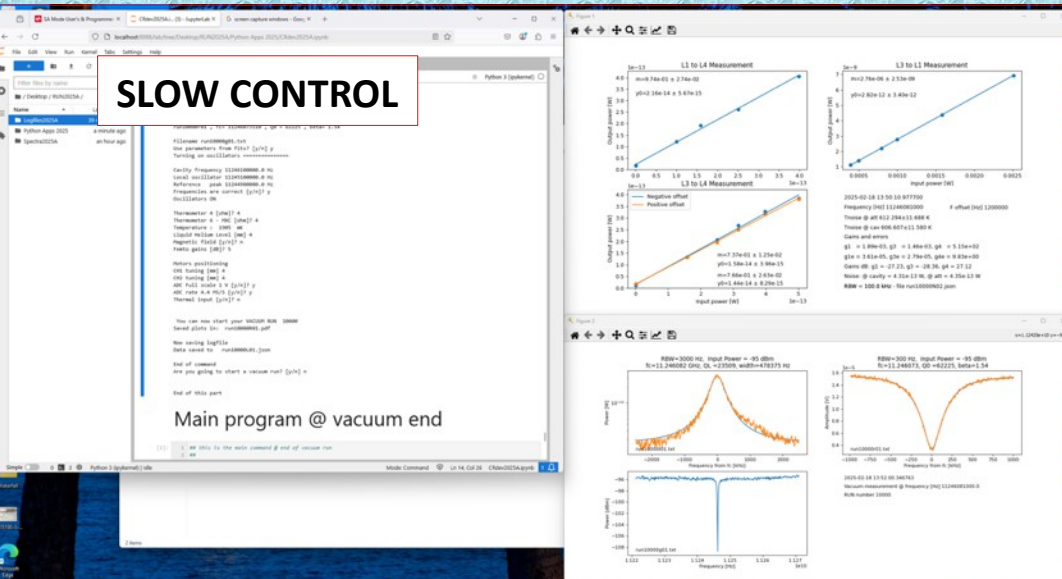
## Noise Temperature Measurement @ every step



Multi-path controller

Original idea published in

A haloscope amplification chain based on a traveling wave parametric amplifier –  
Rev. Sci. Instrum. 2022

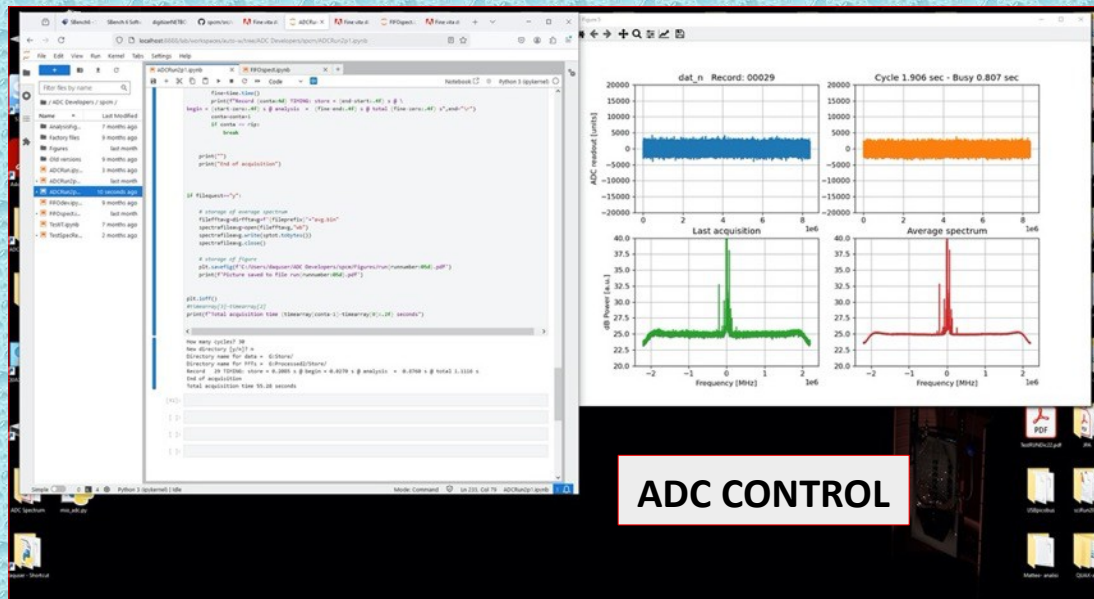
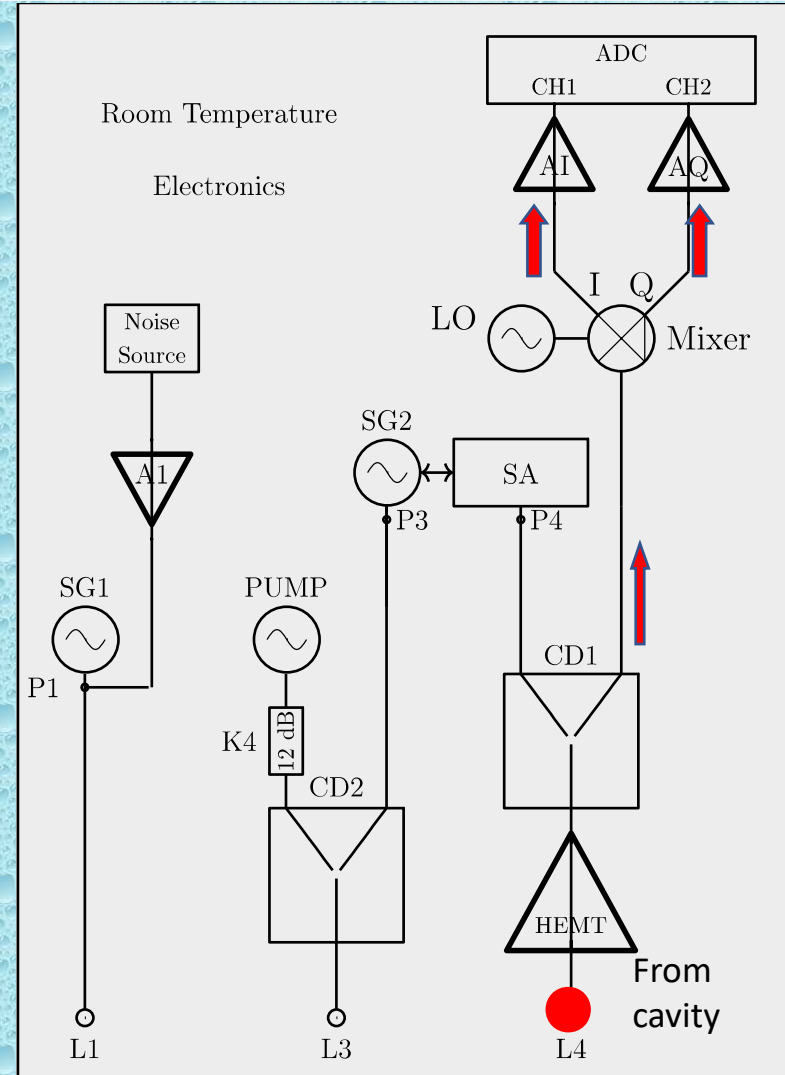


All measured parameters, data and spectra saved to Logfiles

# Data acquisition

- 2- channel acquisition (I, Q from Mixer)
- **Sampling rate = 4.4 MS/s**
- Single block length  $2^{23} = 8\,388\,608$  samples
- Single block length = 1.908 s
- **FFT of each block during acquisition**
- $f_{LO} \sim f_c - 1$  MHz
- Spectral window  $[f_{LO} - 2.2$  MHz,  $f_{LO} + 2.2$  MHz]
- **16384 bins of 268.6 Hz width**

**Raw time data and FFTs stored locally during acquisition**  
**Data copied to cloud once per day**



Data file size 33.6 MByte  
 Typical run 65 GByte  
 Daily request > 1 TByte

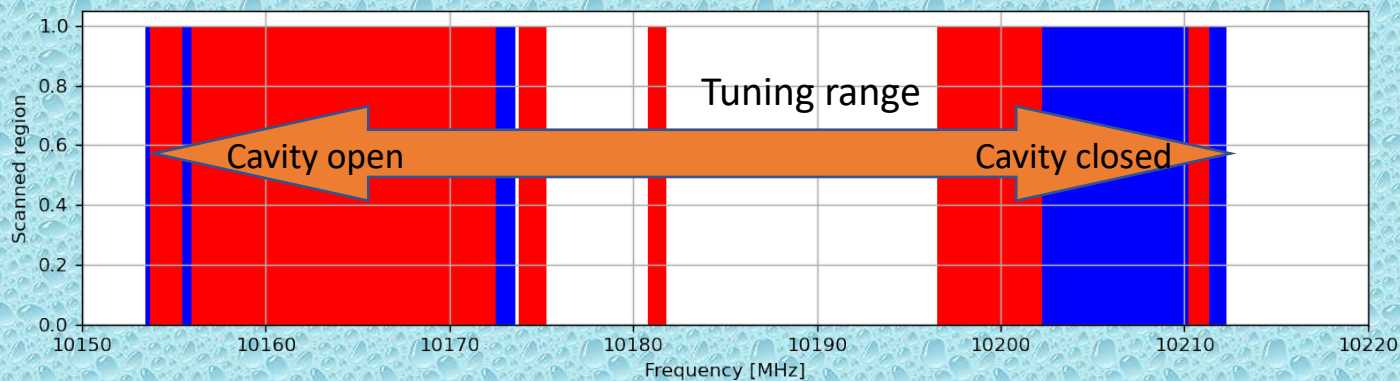
Total memory storage up to about 20 TByte

# QUAX RUN 2024

Magnetic field ON  
Cavity frequency  $f_c = 10.15 - 10.21$  GHz  
Noise temperature  $T_{\text{sys}} = 1.1 - 1.5$  K  
Quality factor  $Q_0 = 60000 - 80000$   
Antenna coupling  $\beta = 1.4 - 1.8$   
Cavity Volume  $V = 1.16$  liters  
Estimated efficiency  $C_{030} = 0.4$   
Effective field  $B^2 = 50.89$  T<sup>2</sup>  
Axion mass  $ma = 44.9$   $\mu\text{eV}$   
Typical Integration time  $t_m = 3800$  s

Expected axion power in a 10 kHz window  $P_a = 6.0e-24$  W

Expected sensitivity (Dicke) in a 10 kHz window  $\sigma_p = 2.5e-23$  W



Spring session

Autumn session

# QUAX RUN 2024 – Spring and autumn sessions

## Spring session

Total run time 3 weeks

2 separate weeks for data taking

May 28th to May 30th - 48 h of field ON

June 11th to June 14th - 90 h of field ON

## Autumn session

Total run time 2 weeks

Nov 7th to Nov 13th - 138 h of field ON

Break due to power failure

Nov 19th to Nov 21th - 42 h of field ON

Covered span:

~40 MHz with 225 h vacuum data taking

Maximum tuning: 58.45 MHz

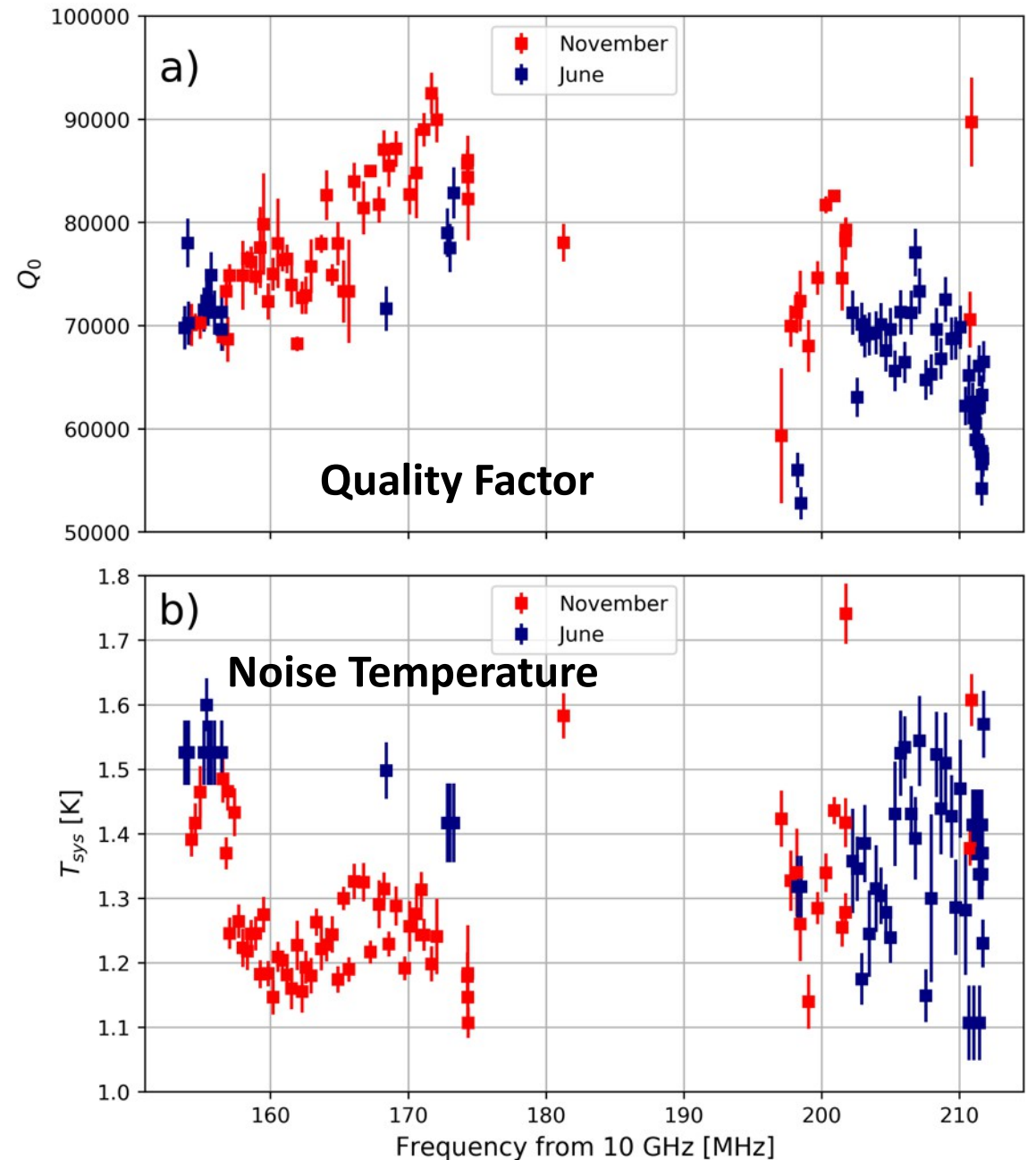
Ratio: 65% of available scan

Duty cycle 50%

Effective scan rate about

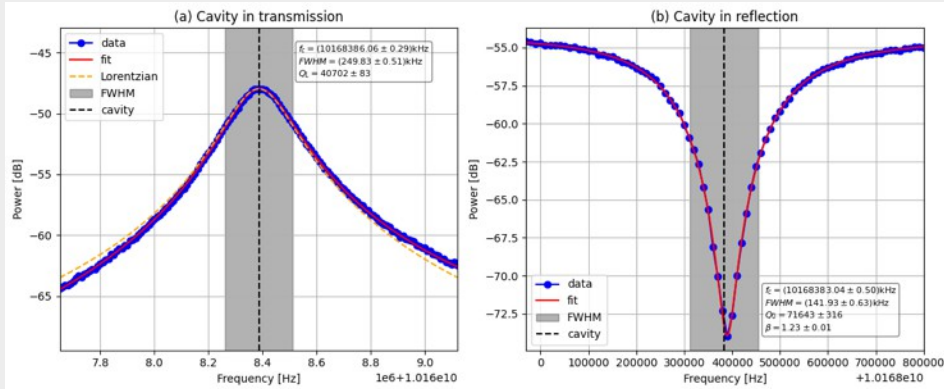
100 kHz/hour

2.5 MHz/day



# Data analysis

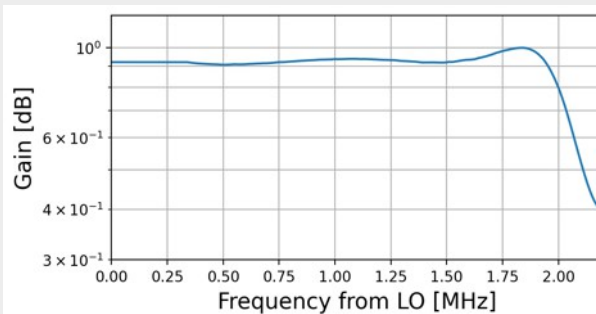
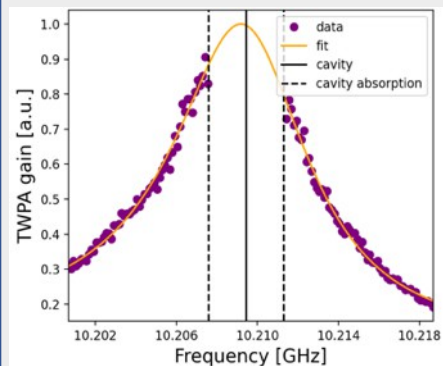
## Parameter evaluation ( $\beta$ , $f_c$ , $Q_0$ , $Q_L$ )



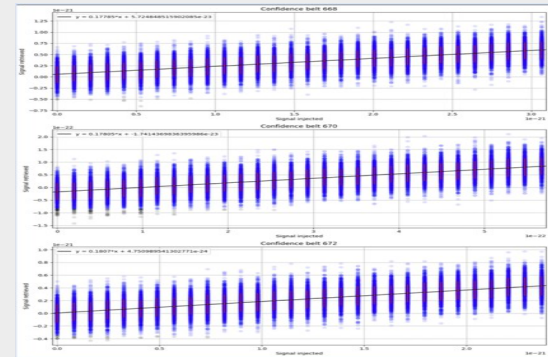
## Remove freq-dependent

TWPA

Filters

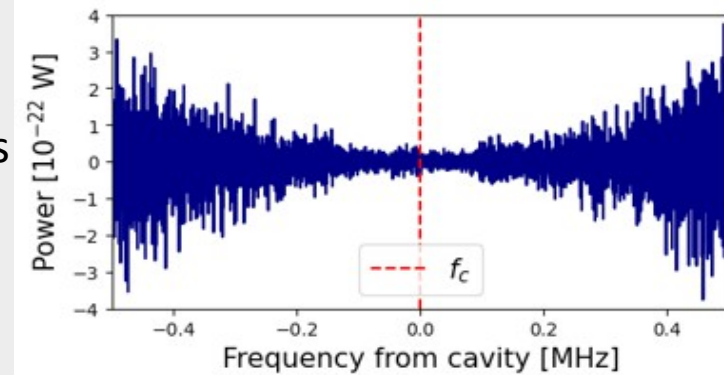


- Average FFT of single frequency steps (bin = 268 Hz)
- Baseline removal with Savitzky Golay filtering
- Monte Carlo simulations to build confidence belts and look for excess power



Digital signal injection

Fluctuations at input



$$P_{\text{in}}^a(\nu, \nu_a) = g_{a\gamma\gamma}^2 \frac{\hbar^3 c^3 \rho_a}{m_a^2} \frac{2\pi\nu_a}{\mu_0} B^2 V C_{030} f_a(\nu, \nu_a)$$

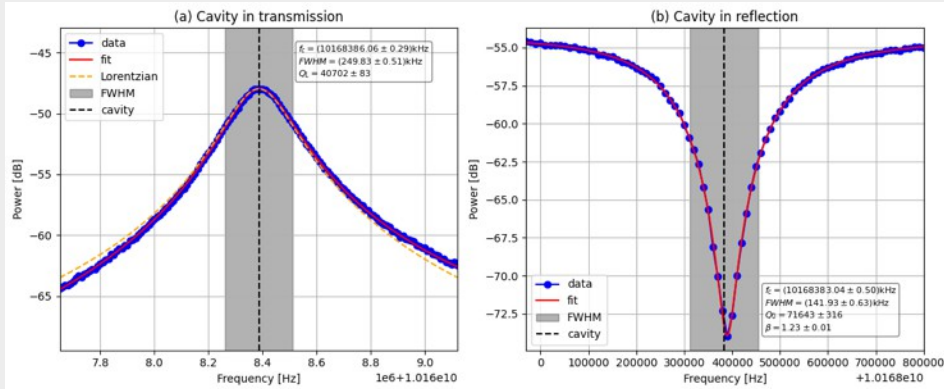
Axion power

$$f_a(\nu, \nu_a) = \frac{2}{\sqrt{\pi}} \sqrt{\nu - \nu_a} \left( \frac{3}{1.7\nu_a \langle \beta_a^2 \rangle} \right)^{3/2} e^{-\frac{3(\nu - \nu_a)}{1.7\nu_a \langle \beta_a^2 \rangle}}$$

Maxwell Boltzmann distribution

# Data analysis

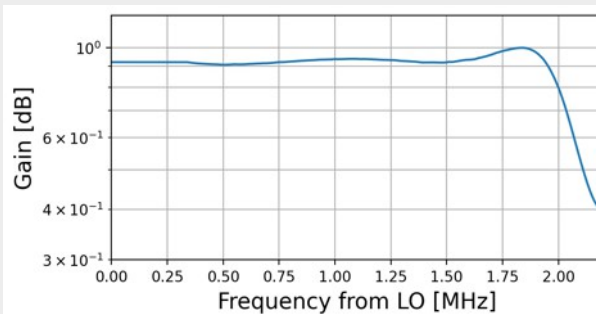
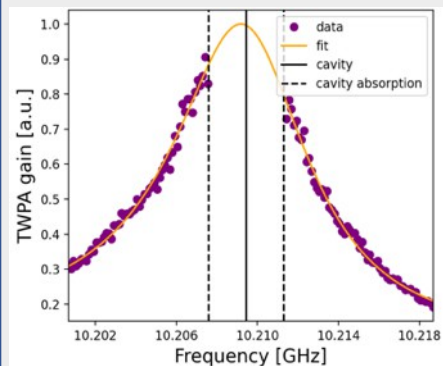
## Parameter evaluation ( $\beta$ , $f_c$ , $Q_0$ , $Q_L$ )



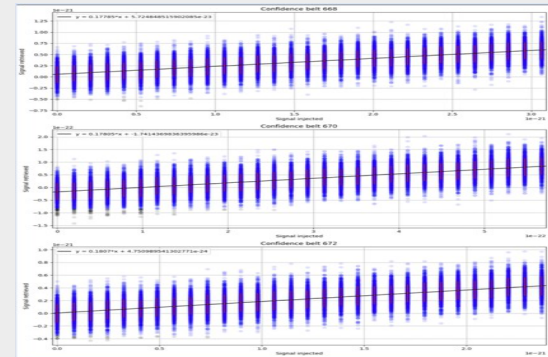
## Remove freq-dependent

TWPA

Filters

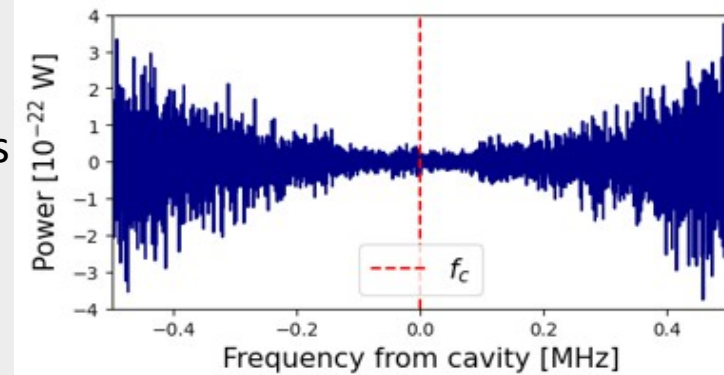


- Average FFT of single frequency steps (bin = 268 Hz)
- Baseline removal with Savitzky Golay filtering
- Monte Carlo simulations to build confidence belts and look for excess power



Digital signal injection

Fluctuations at input



$$P_{\text{in}}^a(\nu, \nu_a) = g_{a\gamma\gamma}^2 \frac{\hbar^3 c^3 \rho_a}{m_a^2} \frac{2\pi\nu_a}{\mu_0} B^2 V C_{030} f_a(\nu, \nu_a)$$

Axion power

$$f_a(\nu, \nu_a) = \frac{2}{\sqrt{\pi}} \sqrt{\nu - \nu_a} \left( \frac{3}{1.7\nu_a \langle \beta_a^2 \rangle} \right)^{3/2} e^{-\frac{3(\nu - \nu_a)}{1.7\nu_a \langle \beta_a^2 \rangle}}$$

Maxwell Boltzmann distribution

# QUAX RUN 2024

No candidate signal have been detected with threshold  $4.5 \sigma$

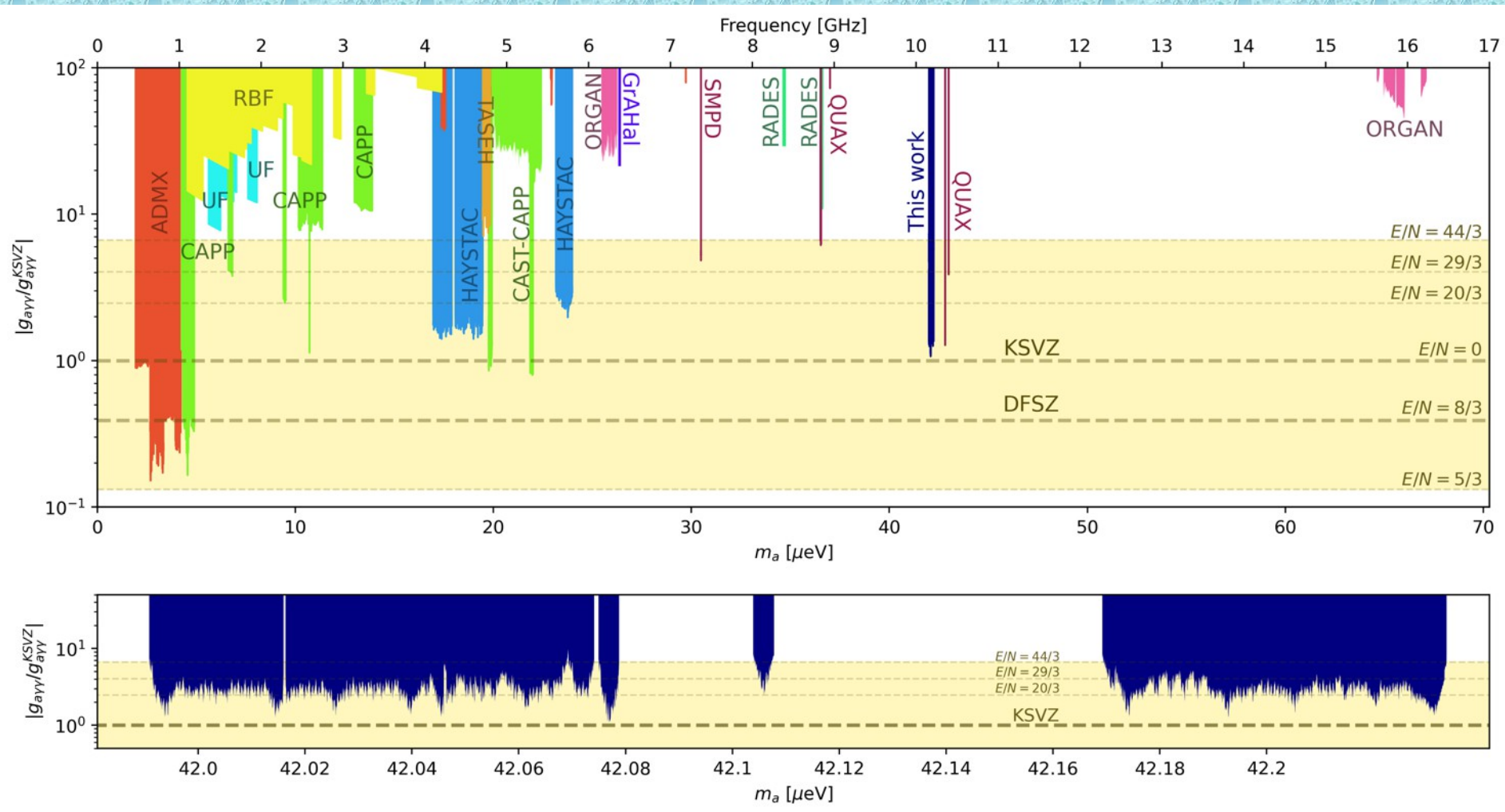
Axion-photon limits at 90% C.L.

PHYSICAL REVIEW LETTERS 135, 211002 (2025)

## Search for Postinflationary QCD Axions with a Quantum-Limited Tunable Microwave Receiver

G. Sardo Infirri<sup>1,2,\*</sup>, D. Alesini<sup>3</sup>, C. Braggio<sup>1,2</sup>, G. Cappelli<sup>4</sup>, G. Carugno<sup>1,2</sup>, D. D'Agostino<sup>5</sup>, A. D'Elia<sup>3</sup>, D. Di Gioacchino<sup>3</sup>, R. Di Vora<sup>6</sup>, M. Esposito<sup>4,†</sup>, P. Falferi<sup>7,8</sup>, U. Gambardella<sup>5</sup>, A. Gardikiotis<sup>1</sup>, C. Gatti<sup>3</sup>, C. Ligi<sup>3</sup>, G. Lilli<sup>6</sup>, A. Lombardi<sup>6</sup>, G. Maccarrone<sup>3</sup>, D. Maiello<sup>1,2</sup>, A. Ortolan<sup>6</sup>, A. Ranadive<sup>4,‡</sup>, A. Rettaroli<sup>3</sup>, N. Roch<sup>4</sup>, S. Tocci<sup>3</sup> and G. Ruoso<sup>6,§</sup>

(QUAX Collaboration)



# Measurement sessions 2025 - 2026

- Major problems with DU unit, reduced machine availability
- Problems now solved!
- No changes on the RF hardware
- Improvement on tuning mechanism to exploit full cavity range
- Improvements on the RF and acquisition system to employ almost full **automatization**

## 2025C session

Total run time 8 days

Nov 13th to Nov 17th - 92 h of field ON  
Scanned about 15 MHz

## 2026A session

Total run time 11 days

April 28th to May 6th - 188 h of field ON  
Scanned about 34 MHz

Covered span 2025 - 2026:

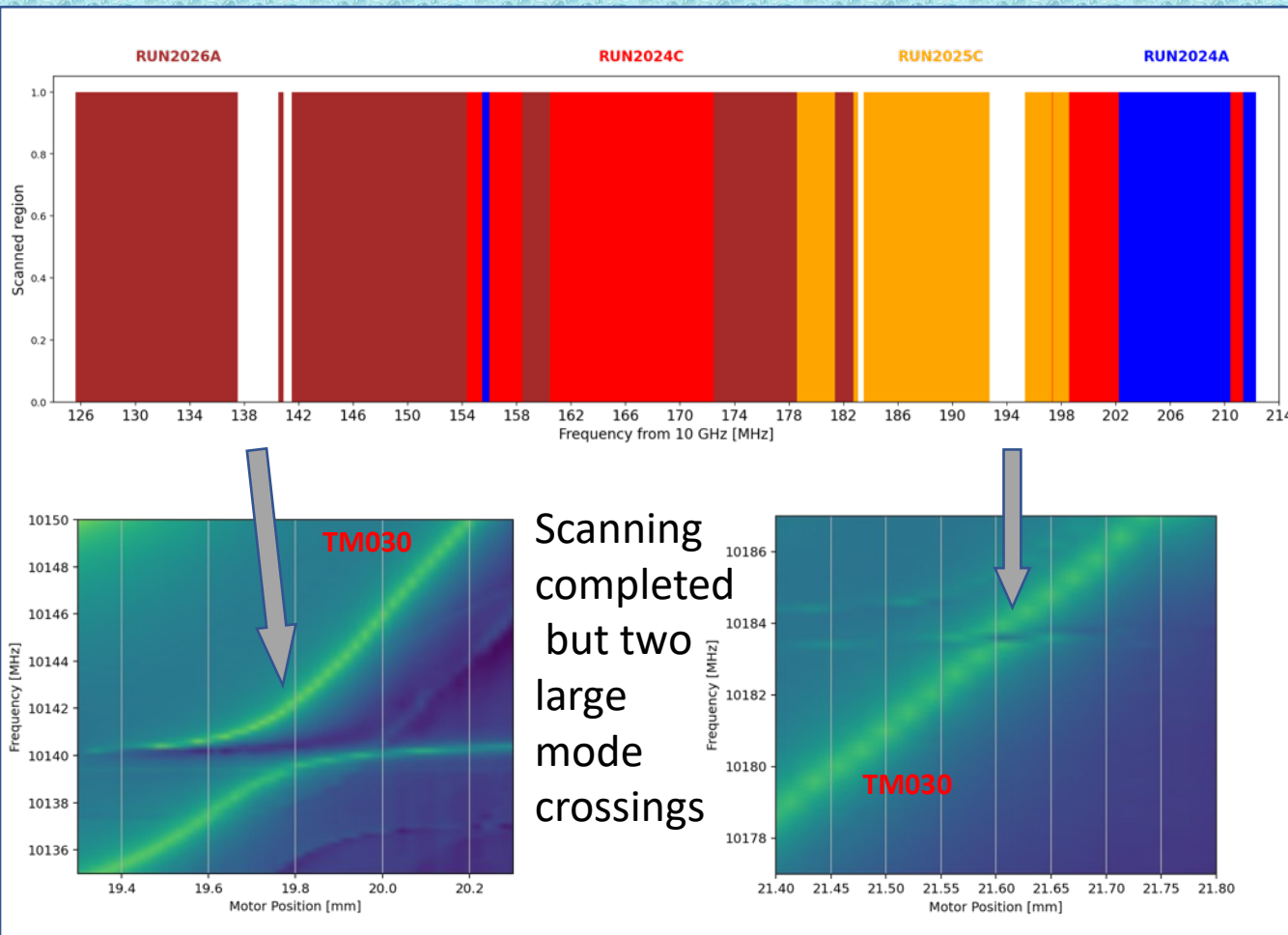
**~49 MHz** with 280 h magnetic field ON

Effective scan rate about

180 kHz/hour

**4.2 MHz/day**

**Data analysis on the way !**

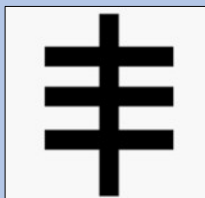


# QUAX – the near future

- Data analysis and check for re-scanning with current cavity
- Install new cavity with larger tuning and increased Q factor

## SAMEK 3G

(Phoenician: Pillar)



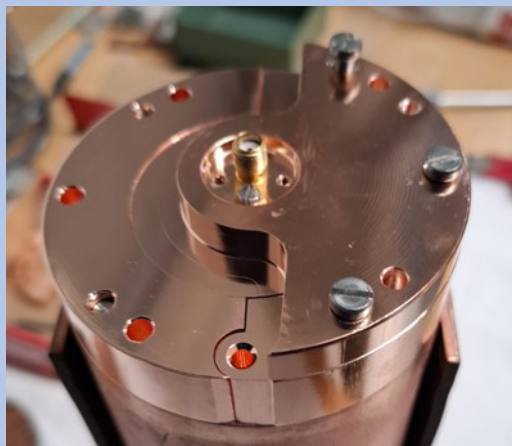
- New endcaps – two sliding parts
- No RF sliding contacts → no friction
- New aperture mechanism

Preliminary results (with short prototype):

tuning range 170 MHz (10.04 – 10.21 GHz)

with  $Q_0 \sim 100\,000 - 130\,000$

Measured  $Q_0 \sim 600\,000$  with  
superconductive walls!



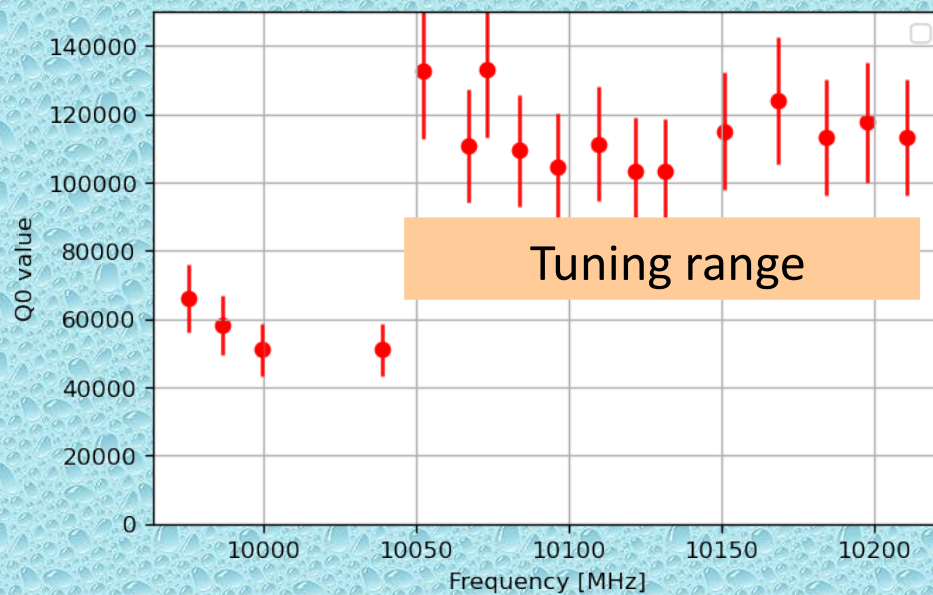
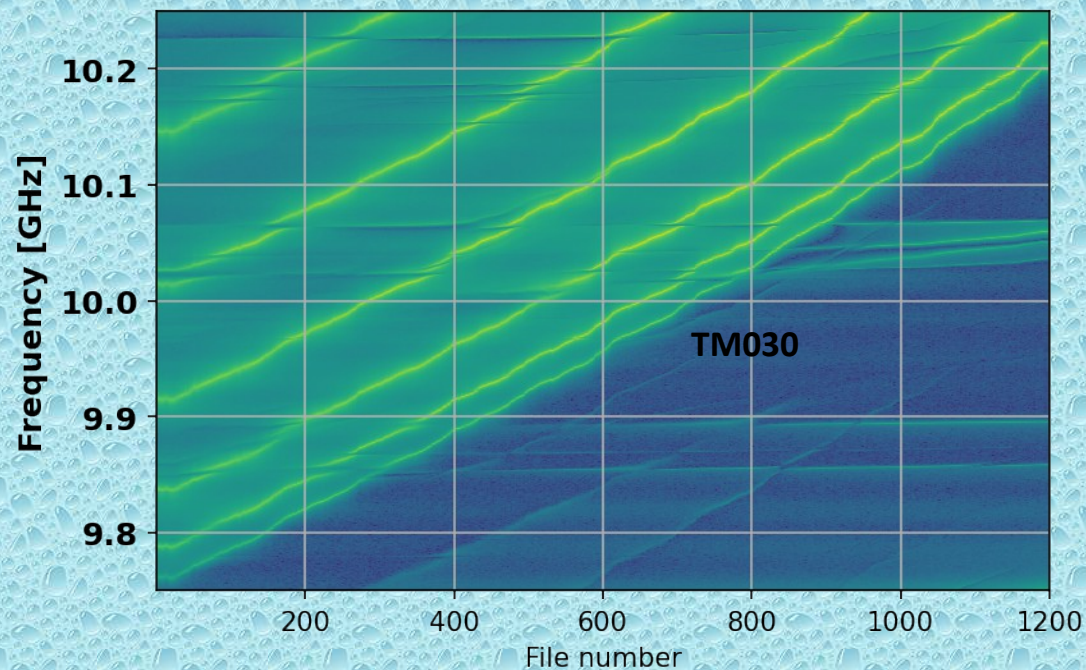
# SAMEK 3G

Short prototype for testing:

Length = 243.4 mm  
Inner diameter 60.5 mm  
Sapphire from Lithuania  
Science mode TM030



Tested @ 4 K



# QUAX @ LNL long term future

Installation of a **14 T magnet**  
Expected summer 2026

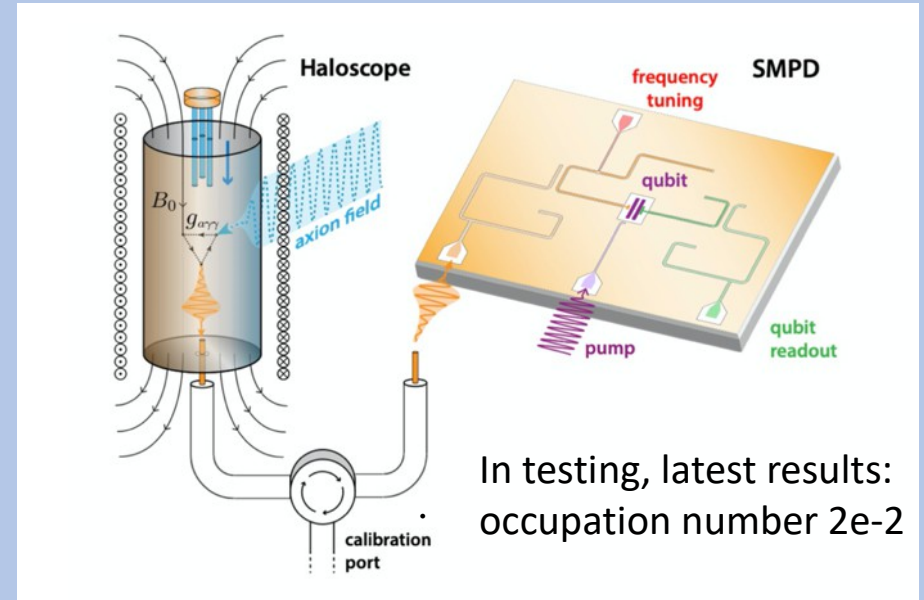


Model	: JMTA-14T103
Coil configuration	: Solenoid coil
Maximum central field	: 14 Tesla
Free bore diameter	: 103 mm
Outer diameter of the solenoid	: 400 mm excluding protrusion (tentative)
Total height of the solenoid	: 500 mm excluding protrusion (tentative)
Total weight (approximately)	: 250 kg (tentative)
Field direction	: Vertical two-way
Operating current (nominal)	: 185 A (tentative)
Inductance	: 64 Henries (tentative)
Maximum sweep rate	: 14 Tesla / 60 minutes (tentative)
Field homogeneity (designed value):	More than 9 Tesla in a cylindrical area of 60mm diameter and 420 mm height



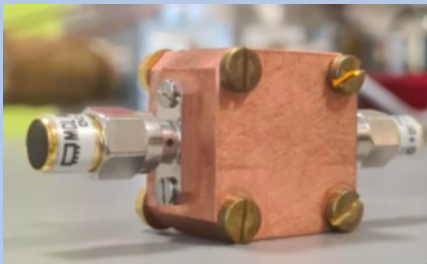
Photo 1 Appearance of JMTA-14T103.

- **Single Photon Microwave Detector (SMPD)** – Help of Qnantronics Group Paris



In testing, latest results:  
occupation number  $2e-2$

First axion run in ferrimagnetic haloscope configuration



**New TWPA**  
amplifier from  
Grenoble  
optimized for 10  
– 11 GHz band

Large bandwidth (7.6-8.7 GHz), high Q ( $>2e6$ )

- **dark photon search...** data analysis in progress

- Installation of **new cryogenic system**
  - Wet assembly with reliquefier for magnet
  - Dry unit for cavity and RF detection

This will allow for longer and safer operation

- Develop high Q, high volume cavities based on **High Temperature Superconductor (ReBCO)**

# People

## QUAX Padova / Legnaro



F. Calaon

G. Ruoso, R. Di Vora, E. Berto, G. Carugno, A. Lombardi

C. Braggio

M. Tessaro



D. Ahn, D. Maiello, A. Ortolan

G. Sardo Infirri



## QUAX Frascati

D. Alesini, A. D'Elia, D. Di Gioacchino, C. Gatti, C. Ligi, G. Maccarrone, A. Rettaroli, and S. Tocci

## QUAX Grenoble

G. Cappelli, M. Esposito, A. Ranadive, N. Roch

## QUAX Trento

P. Falferi

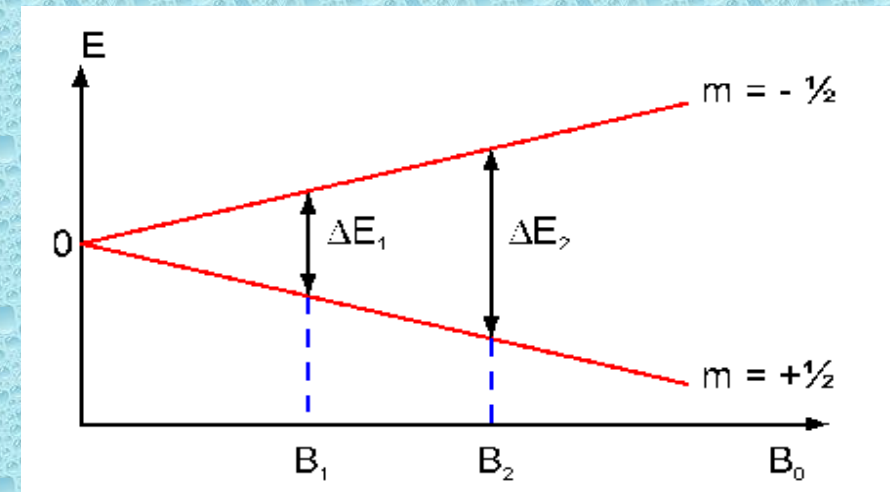
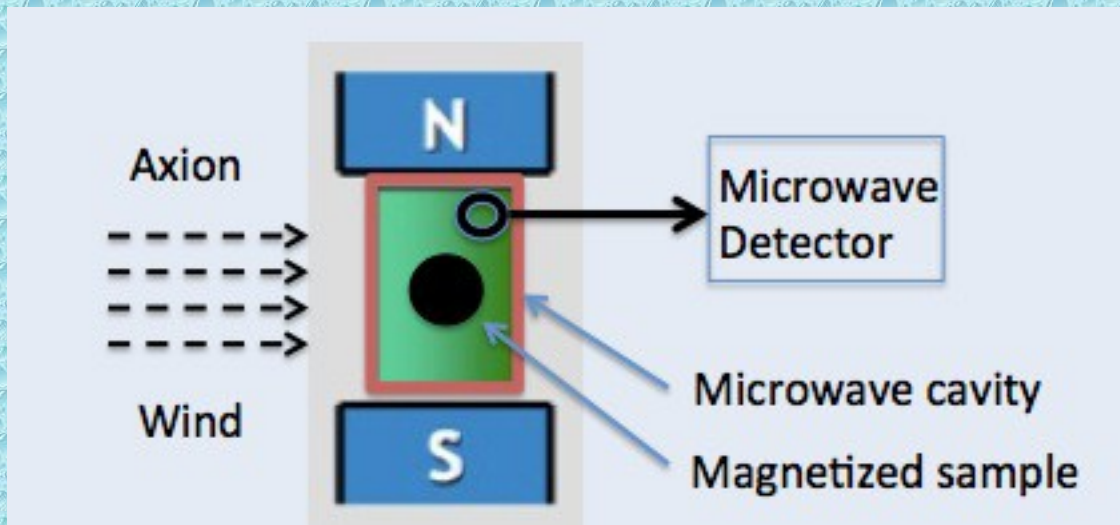
## QUAX Salerno

U. Gambardella, D. D'Agostino

# Supplementary slides

# The ferrimagnetic QUAX: sensing the axion wind

- **Due to the motion of the solar system** in the galaxy, the axion DM cloud acts as an **effective RF magnetic field on electron spin**
- This field excites **magnetic transition in a magnetized sample** (Larmor frequency) and produces a detectable signal

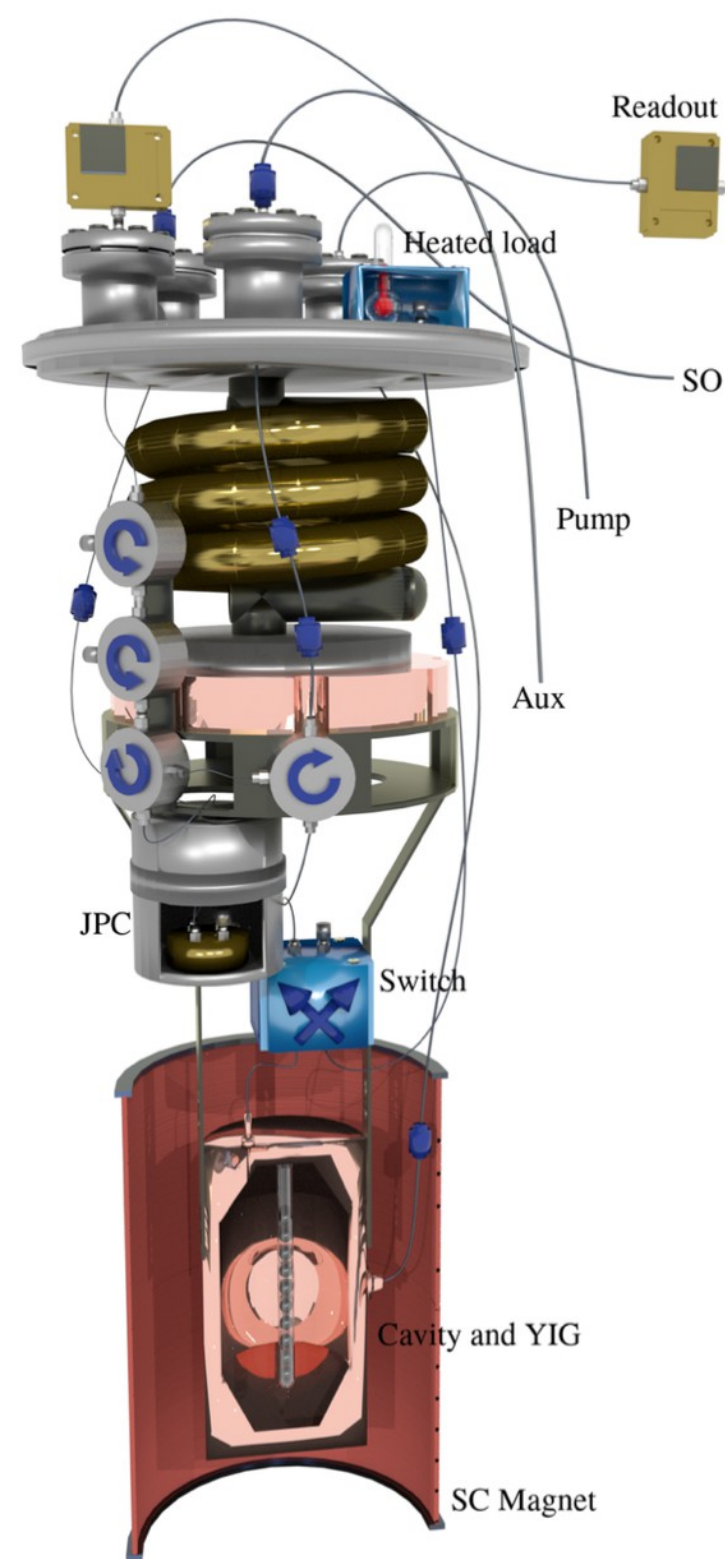
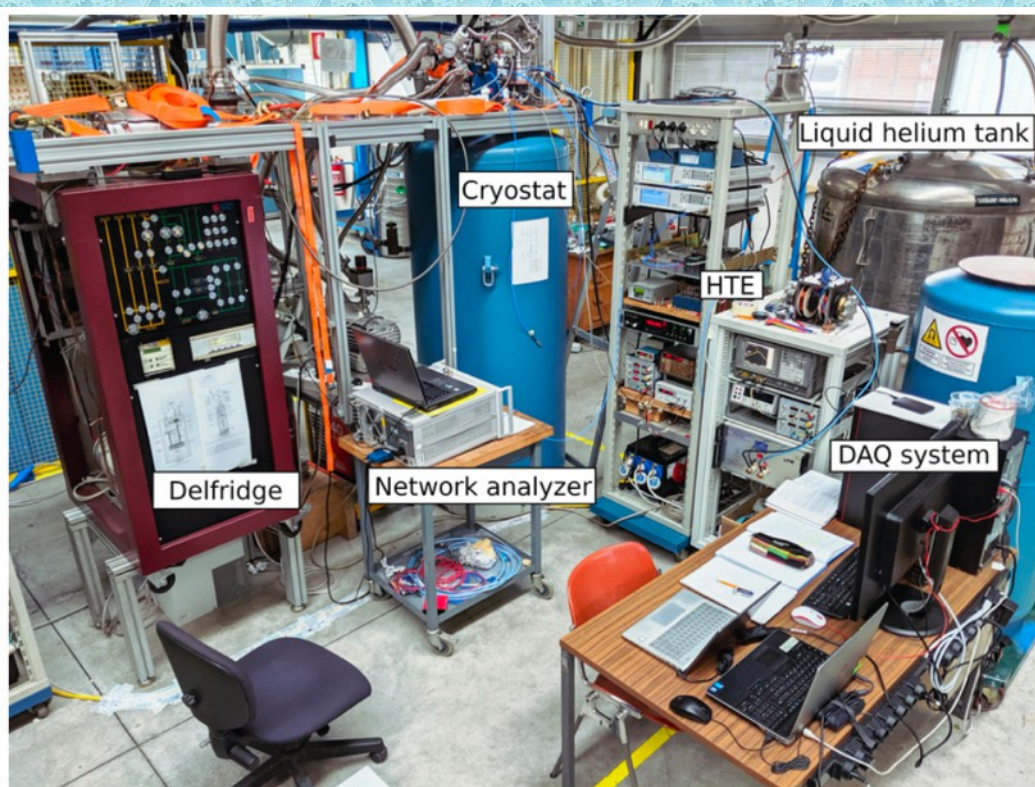


Idea comes from **several old works**:

- L.M. Krauss, J. Moody, F. Wilczek, D.E. Morris, "Spin coupled axion detections", HUTP-85/A006 (1985)
- R. Barbieri, M. Cerdonio, G. Fiorentini, S. Vitale, Phys. Lett. B 226, 357 (1989)
- F. Caspers, Y. Semertzidis, "Ferri-magnetic resonance, magnetostatic waves and open resonators for axion detection", Workshop on Cosmic Axions, World Scientific Pub. Co., Singapore, p. 173 (1990)
- A.I. Kakhizde, I. V. Kolokolov, Sov. Phys. JETP 72 598 (1991)

# Ferrimagnetic QUAX

- **Large volume**  
10 YIG sphere 2.1 mm diameter
- **Reduced noise**  
Quantum limited amplifier (JPC)  
Dilution refrigerator (100 mK)
- **Scan axion mass range**  
Magnetic field tuning



# Results

- FFT the data with a 100 Hz resolution bandwidth to identify and remove biased bins and disturbances

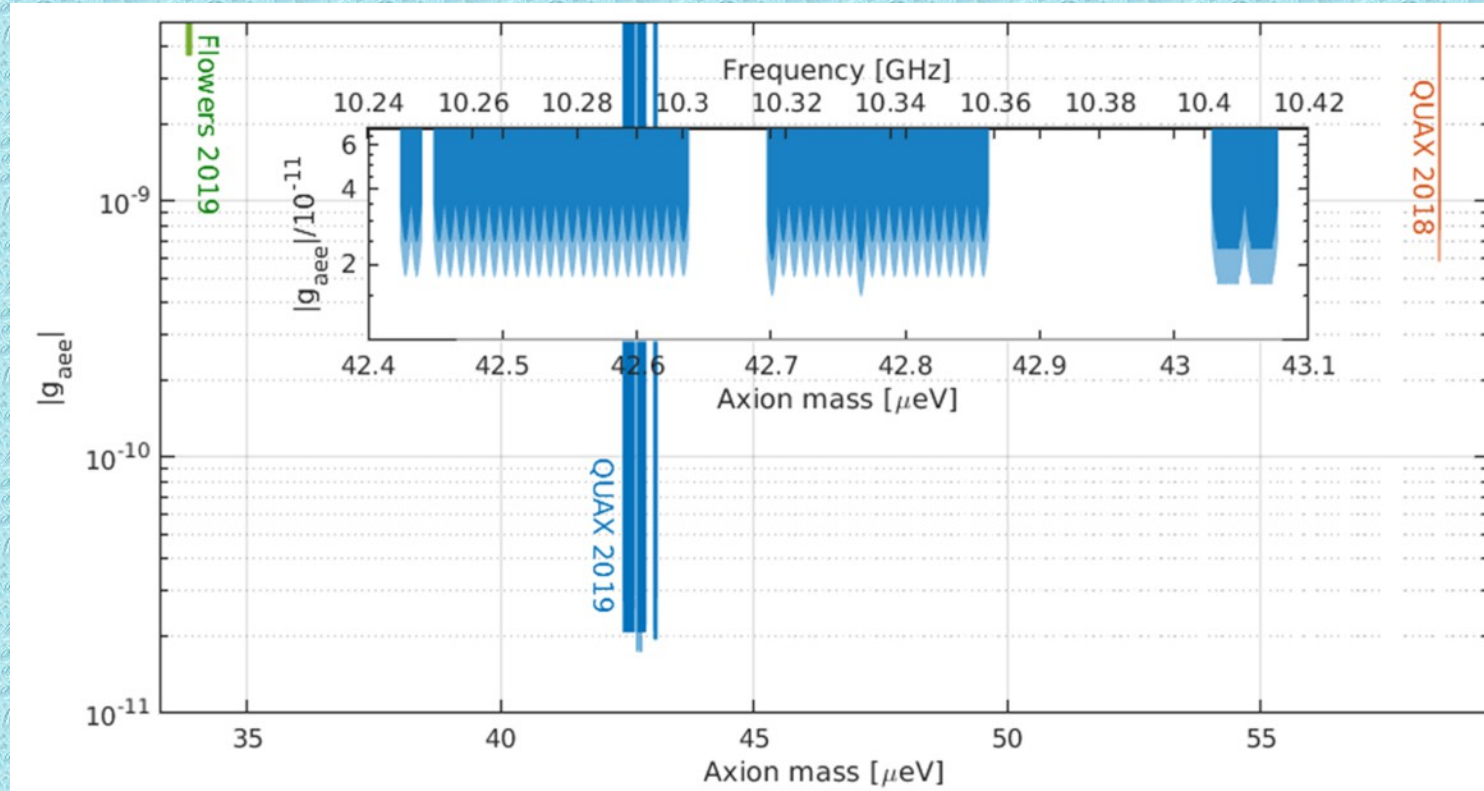
$$g_{aee} < \frac{e}{\pi m_a v_a} \sqrt{\frac{k_{ac} \times 2\sigma_p}{2\mu_B \gamma_e n_a N_s \tau_s}}$$

- Rebin the FFTs with a resolution bandwidth **RBW**  $\approx$  **5 kHz** to look for axion signal

- Look for fluctuations from thermal spectrum

- **The measured fluctuations  $\sigma_p$  compatible with the estimated noise in every run**

- **Assuming DM is 100% made by ALPs ->> 95% CL plot**



PRL **124**, 171801 (2020)

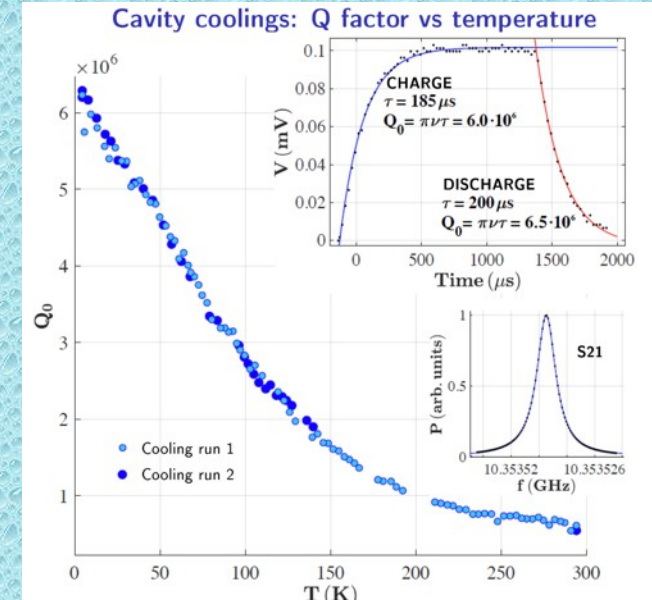
For the longest run (9 h)

best power sensitivity  $\sigma_p = 5.1 \cdot 10^{-24} \text{ W} \rightarrow$  Axion effective field  $B_a = 5.5 \cdot 10^{-19} \text{ T}$

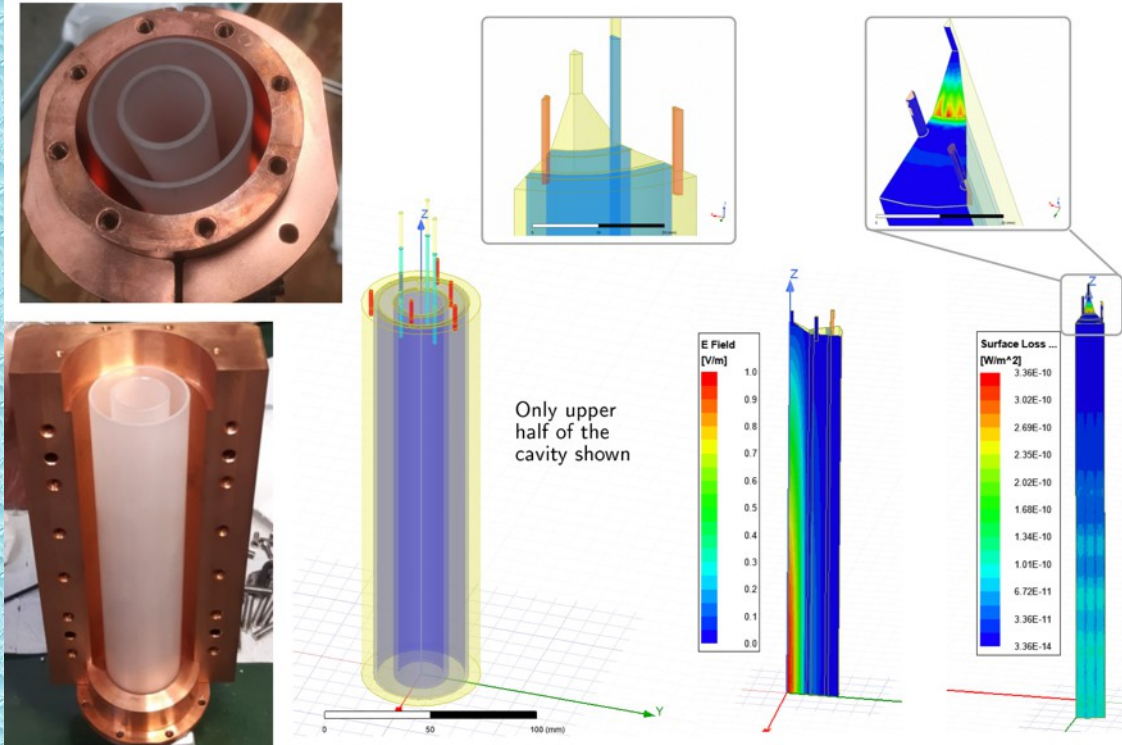
# Dielectrically loaded cavity – High Q

First realization of a **copper cavity dielectrically loaded with two concentric sapphire cylinders** to operate in a strong magnetic field

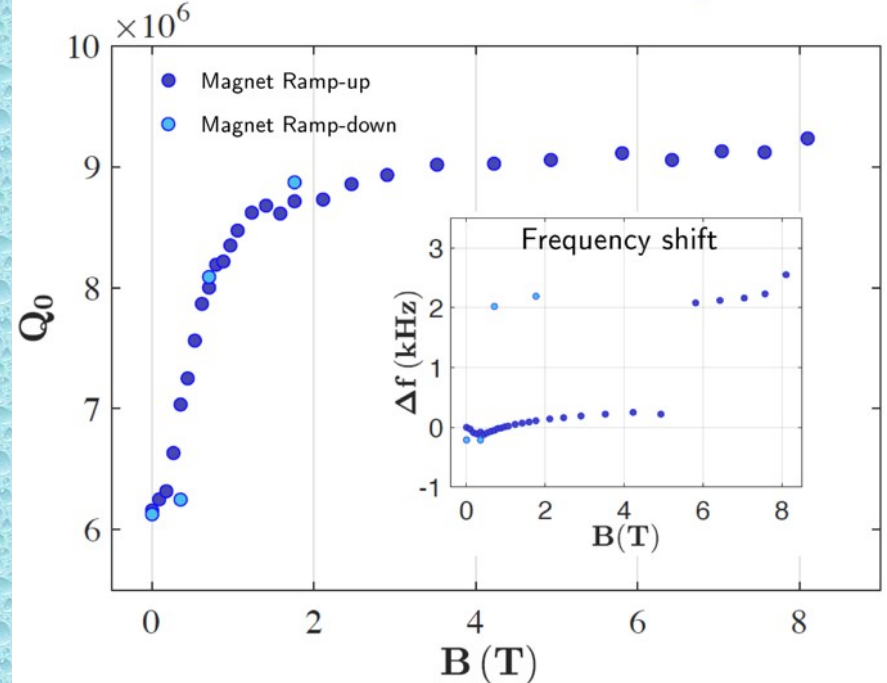
Exceptional Q value  $\sim 10$  Million in an 8 T field



Electric field and surface loss for the TM<sub>030</sub> mode



Measurement at 4 K: Q factor vs magnetic field



- Limited tuning of  $\sim 1.5$  MHz
- Poor coupling to axion field  $C_{030} = 0.034$

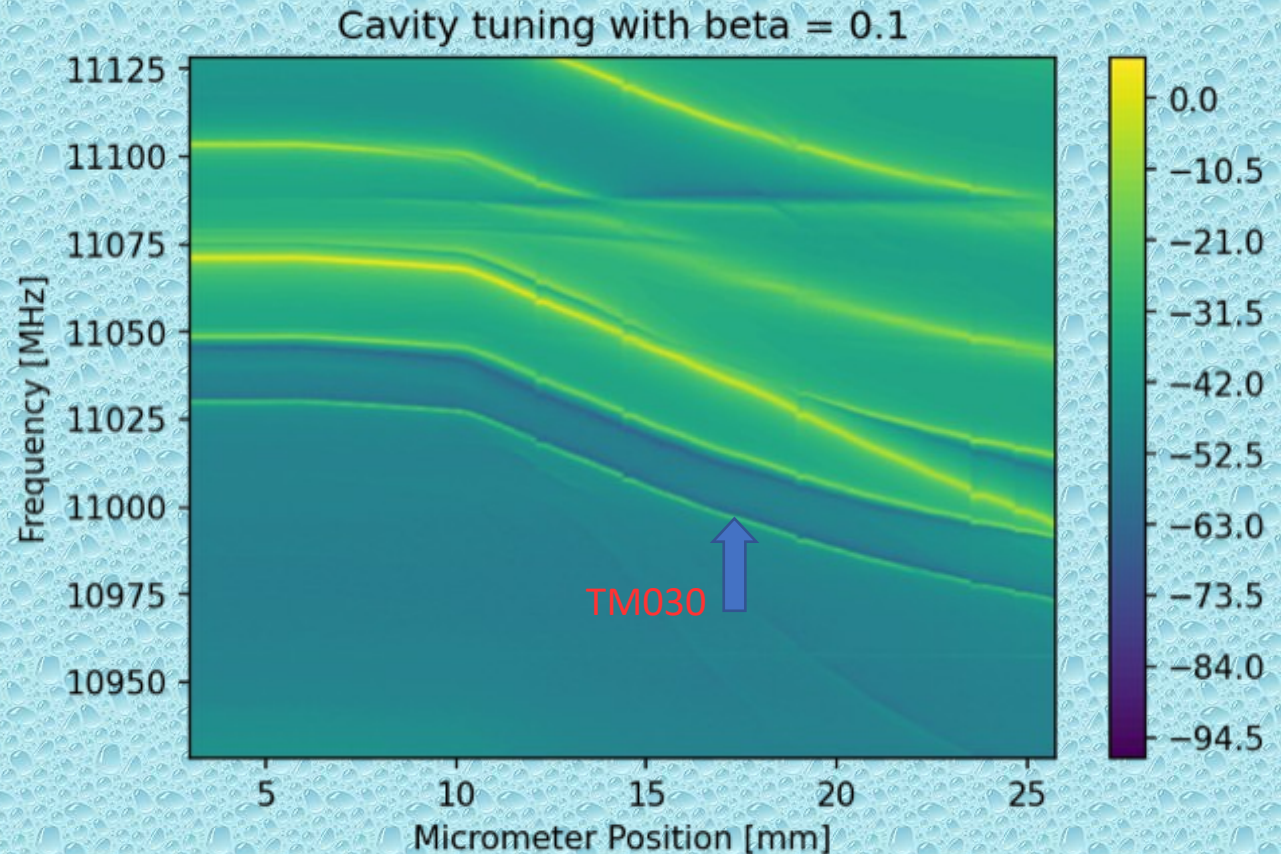
# LNL Haloscope – High Frequency Tunable Cavities

## Objectives:

- Resonance frequency above 10 GHz
- Tunable with range 100 MHz
- Large Volume
- High Q over the entire tuning range
- Limited spurious modes
- Operation in strong B field
- Good coupling to axion field (C factor)
- Bead pulling measurements



**Dedicated test station for cavity characterization @ 4 K**



**Prototype test with thinner sapphire:**

$Q_0 \sim 200\,000$

**Maximum tuning  $\sim 100$  MHz**

## QUAX publications on cavities

- A new class of axion haloscope resonators: the polygonal coaxial cavity – PRApplied, 23, 034047 (2025)
- A tunable large volume dielectric cavity at 11 GHz – Rev. Sci. Instrum. 96, 085204 (2025)
- A tunable clamshell cavity for wavelike dark matter searches - RSI 2023
- High- Q Microwave Dielectric Resonator for Axion Dark-Matter Haloscopes - PRAppl 2022
- Realization of a high quality factor resonator with hollow dielectric cylinders for axion searches - NIMA 2021
- High quality factor photonic cavity for dark matter axion searches - RSI 2020

# TWPA performance

ARTICLE

NATURE COMMUNICATIONS | <https://doi.org/10.1038/s41467-022-29375-5>

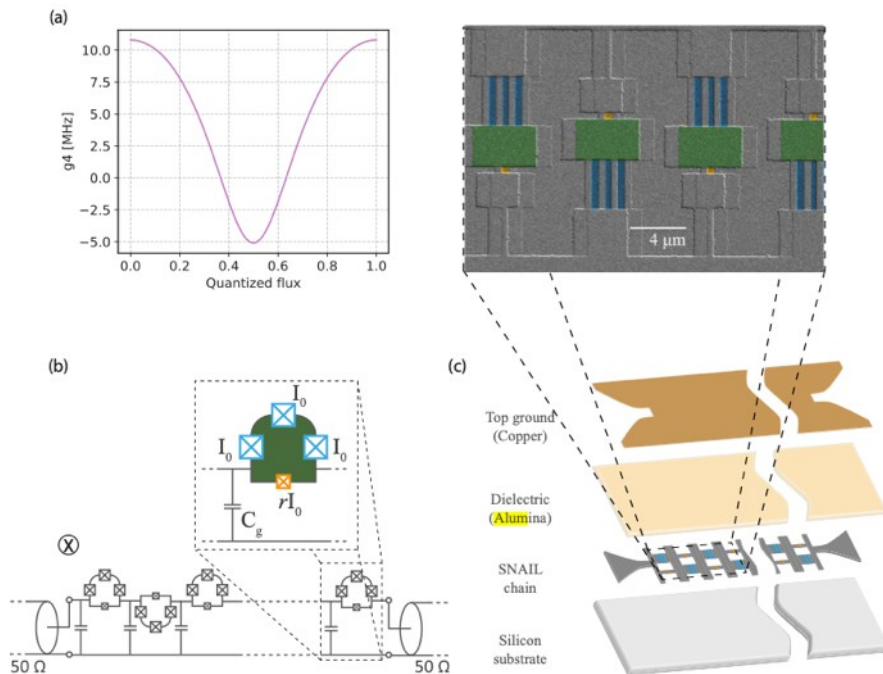
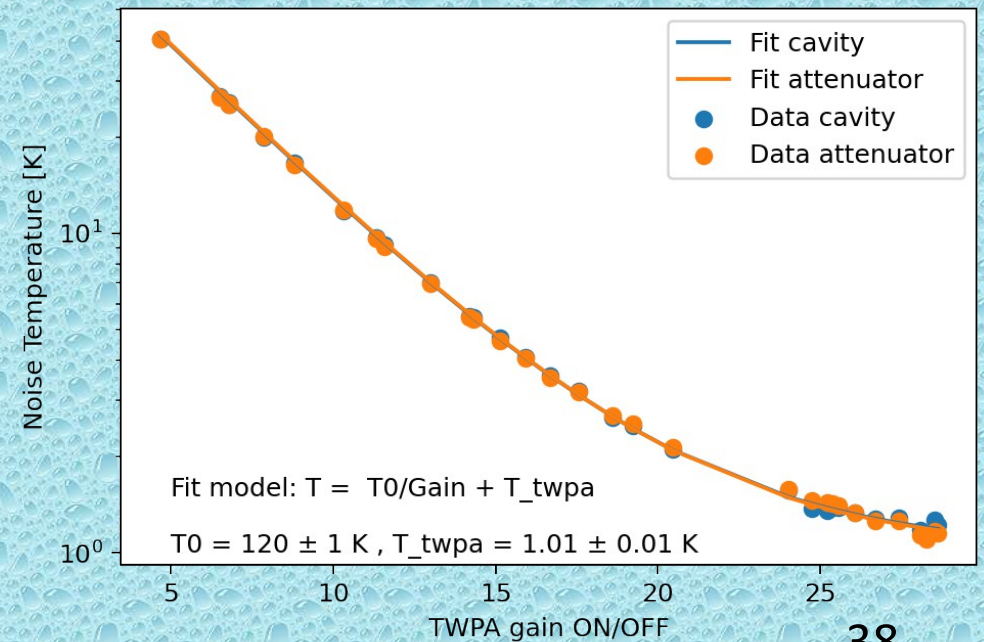
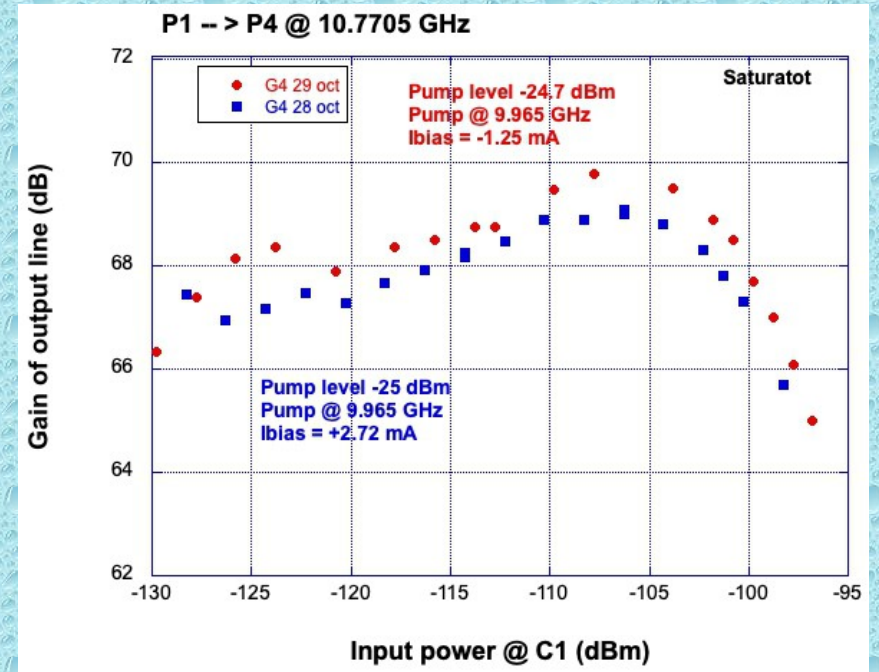
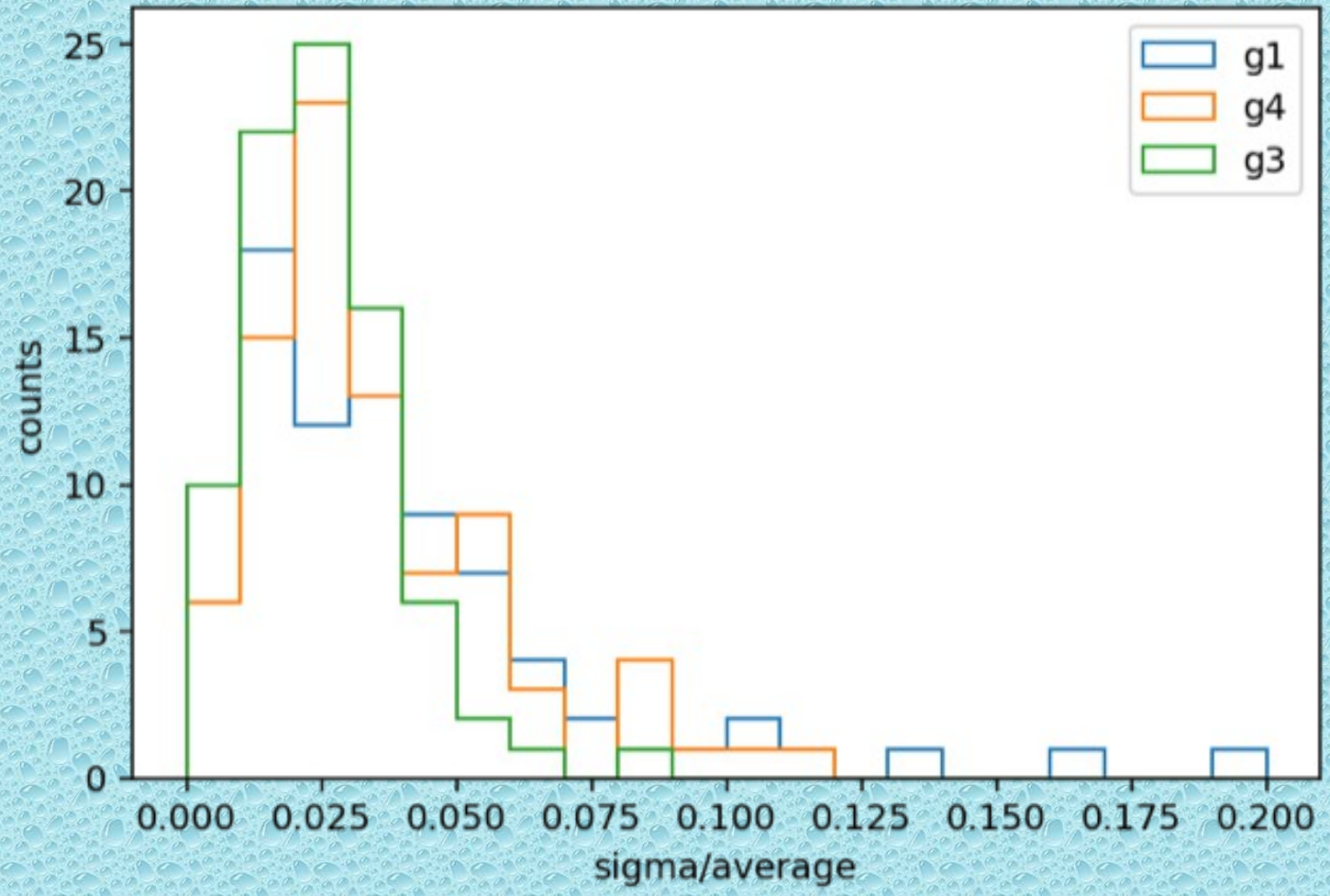


**Fig. 2 Reversed Kerr TWPA implementation.** **a** Nonlinear coefficient  $g_4$  as a function of the external magnetic flux, calculated using the device parameters obtained from the linear characterization ( $I_0 = 2.19 \mu\text{A}$  and  $r = 0.07$ , see supplementary information). **b** Circuit schematic of the reversed Kerr TWPA;  $I_0$  is the critical current of the large junction,  $rI_0$  is the critical current of the small junction and  $C_g$  is the ground capacitance per unit cell. The device is threaded by a global magnetic field. The alternated loop geometry hence results in an alternated magnetic flux polarity. **c** Schematic of the reversed Kerr TWPA. The device is fabricated with double angle aluminum Josephson junction array deposition on silicon substrate, followed by atomic layer deposition of dielectric (alumina) and finally by gold top ground deposition<sup>51</sup>. A scanning electron microscopy (SEM) image of the meta-material with false coloring to indicate large (blue) and small (orange) junctions forming a SNAIL in the transmission line is shown as a closeup; the superconducting loop area is colored green.



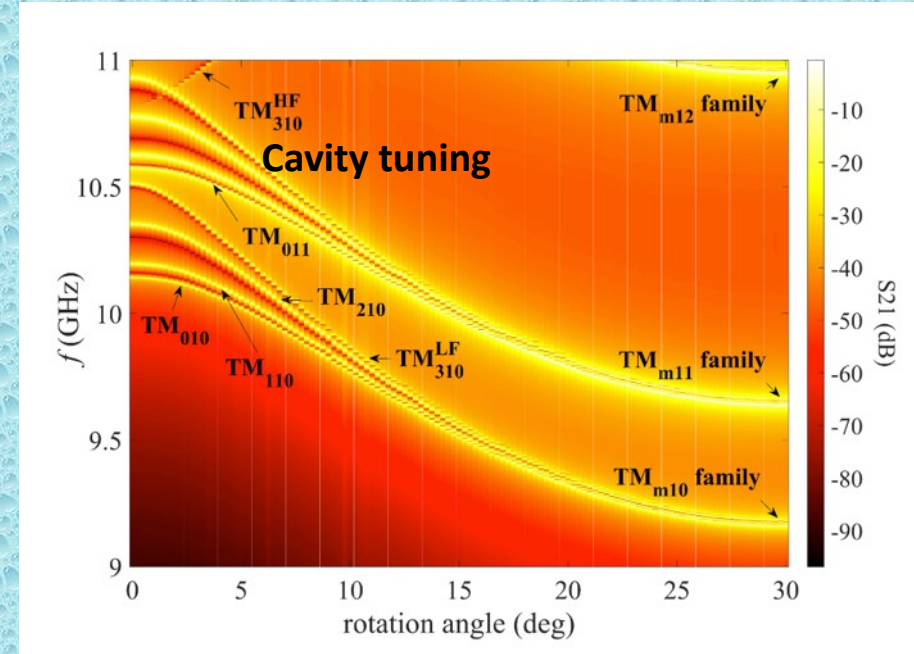
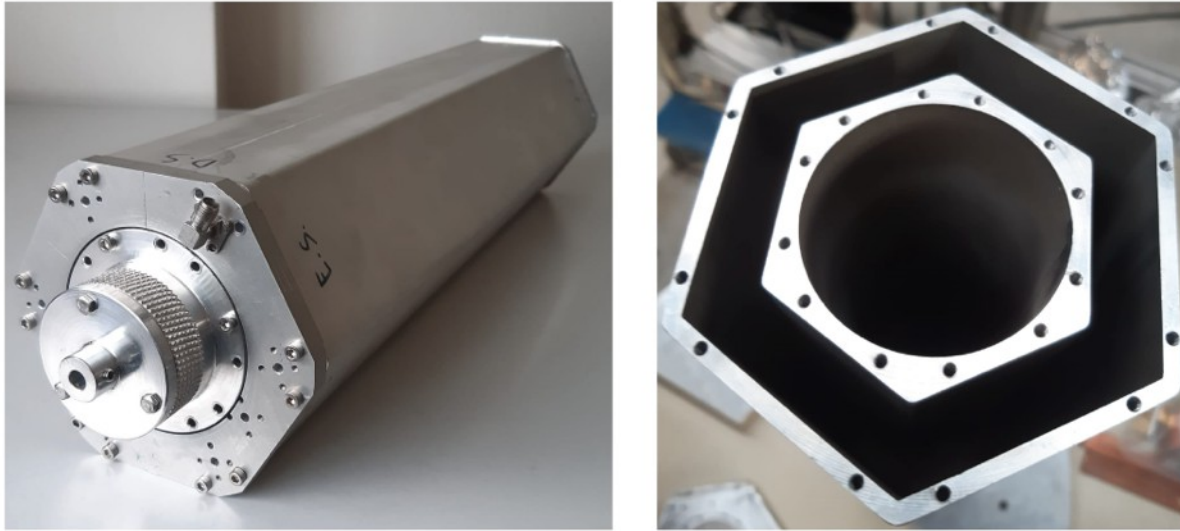
# Noise temperature measurements accuracy

Measurement of the gains  $g_1$ ,  $g_3$ ,  $g_4$  of the RF lines L1, L3, L4



# LNL Haloscope – High Frequency Tunable Cavities

A new class of axion haloscope resonators:  
the polygonal coaxial cavity



For  $L = 420$  mm effective volume = 2 liters \* 0.8 = 1.6 liters

Available tuning about 5% of maximum frequency

